UNITED NATIONS EDUCATIONAL, SCIENTIFIC AND CULTURAL ORGANIZATION
INTERNATIONAL ATOMIC ENERGY AGENCY
INTERNATIONAL CENTRE FOR THEORETICAL PHYSICS

SMR/917 - 32

SECOND WORKSHOP ON
SCIENCE AND TECHNOLOGY OF THIN FILMS

(11 - 29 March 1996)

" Amorphous and microcrystalline silicon-based solar cells "

presented by:

S. GUHA
United Solar Systems Corp.
1100 West Maple Road
MI 48084 Troy
U.S.A.

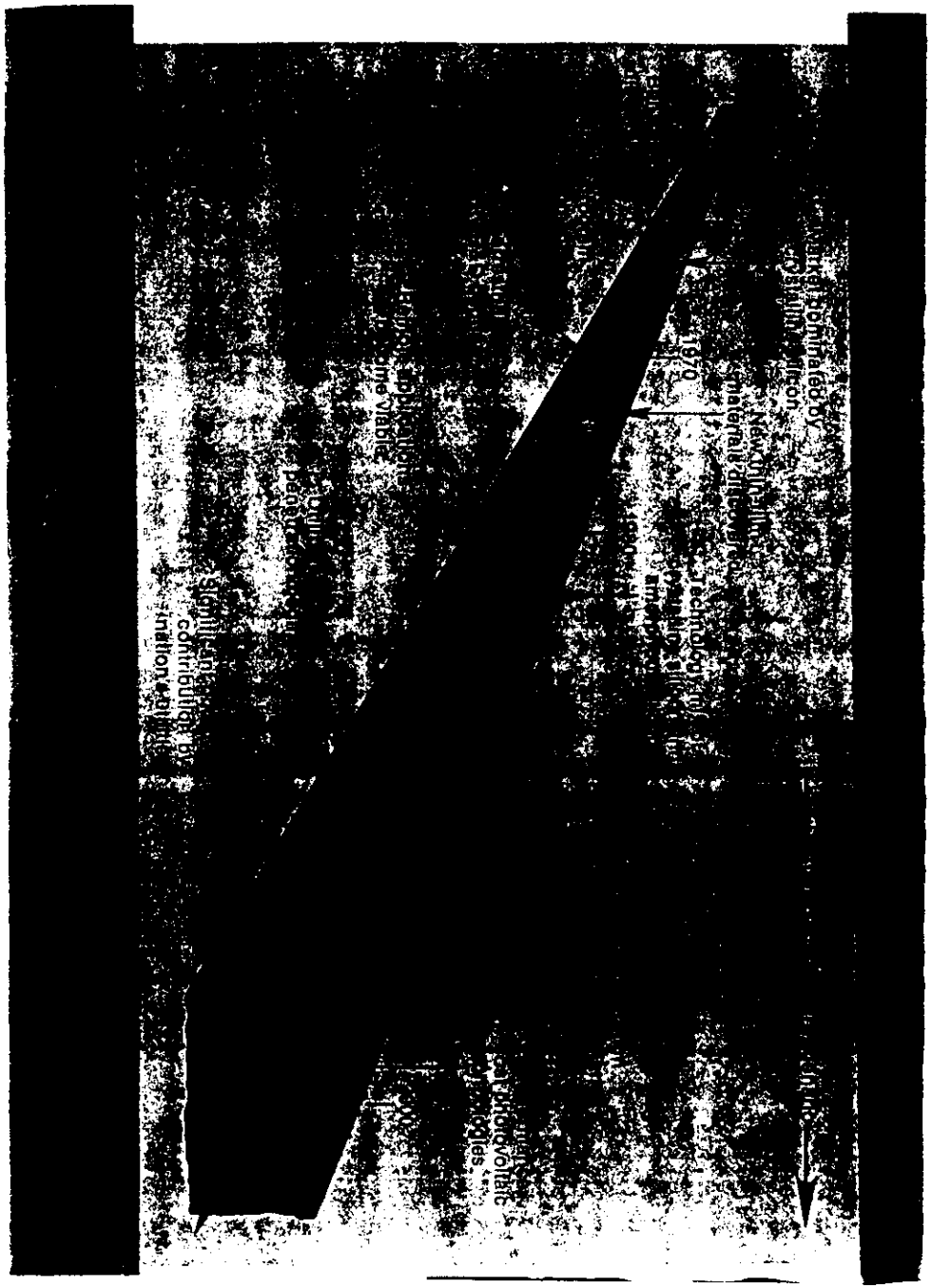

GROWTH OF MAJOR APPLICATIONS

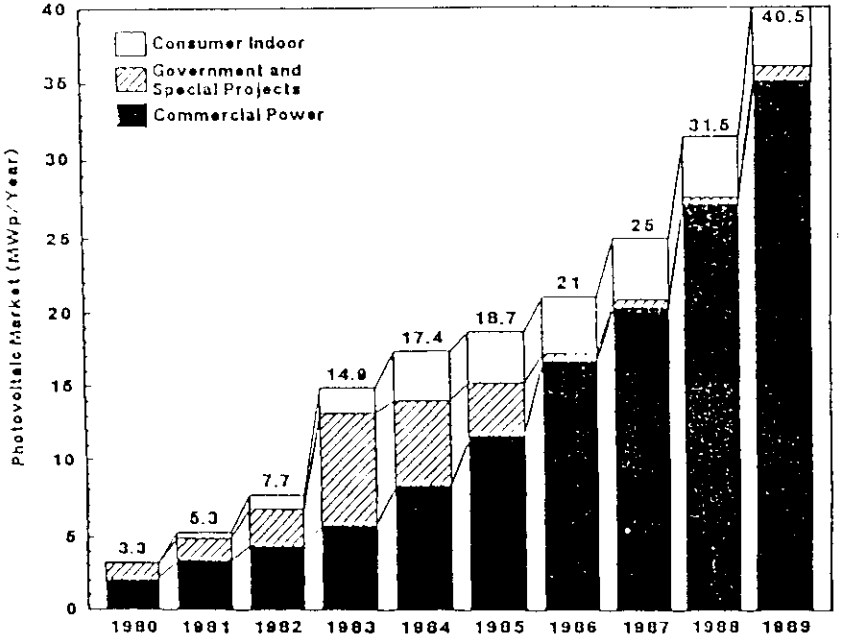

$62 M

$280 M

PHOTOVOLTAIC MARKET

1989	40.5 MW
1990	46.5 MW
1991	55 MW
1992	60 MW
1993	64 MW
1994	70 MW
2000 (F)	300-600 MW

F → FORECAST

REDUCTION OF MODULE COST IS KEY TO ACHIEVING THE INCREASED MARKET GOALS

SELECTION OF MATERIAL

- MANY OPTIONS -- SINGLE CRYSTAL SILICON, POLY-SILICON, THIN FILM AMORPHOUS SILICON.
  ALSO, CADMIUM TELLURIDE, COPPER INDIUM DISELENIDE, GALLIUM ARSENIDE.

ECONOMICS OF PHOTOVOLTAICS

KEY INGREDIENTS

- LOW MATERIAL COST
- HIGH EFFICIENCY WITH GOOD STABILITY
- LOW PROCESSING COST
- HIGH YIELD
- ENVIRONMENTALLY SAFE

It is important to note that <u>all</u> these requirements need to be fulfilled to make PV economically viable

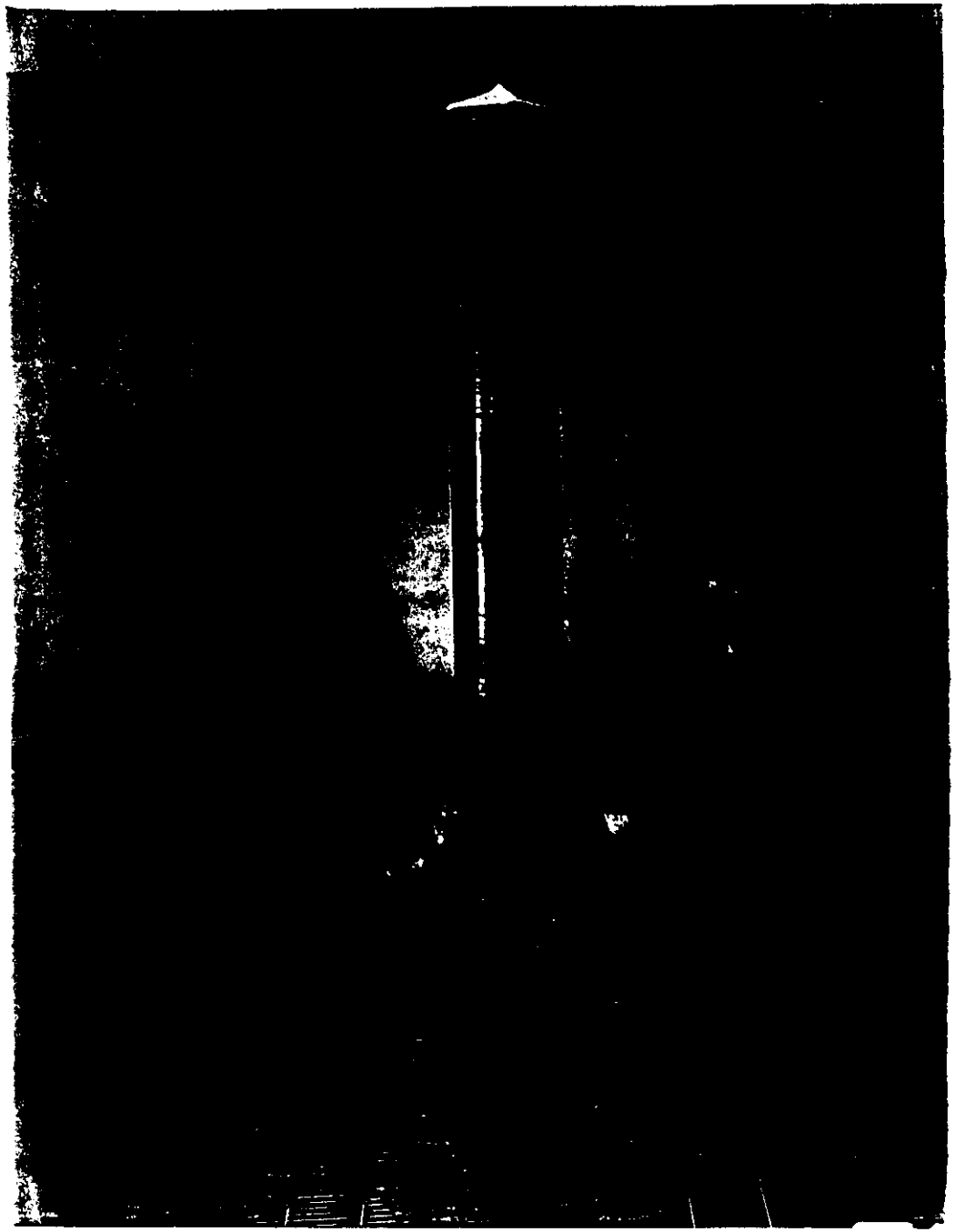

SINGLE CRYSTAL SILICON TECHNOLOGY

- GROW SINGLE CRYSTAL (SOLID ROD)
- CUT INTO SLICES
- VARIOUS PROCESSING STEPS
- CONNECT TOGETHER

  → LARGE COST

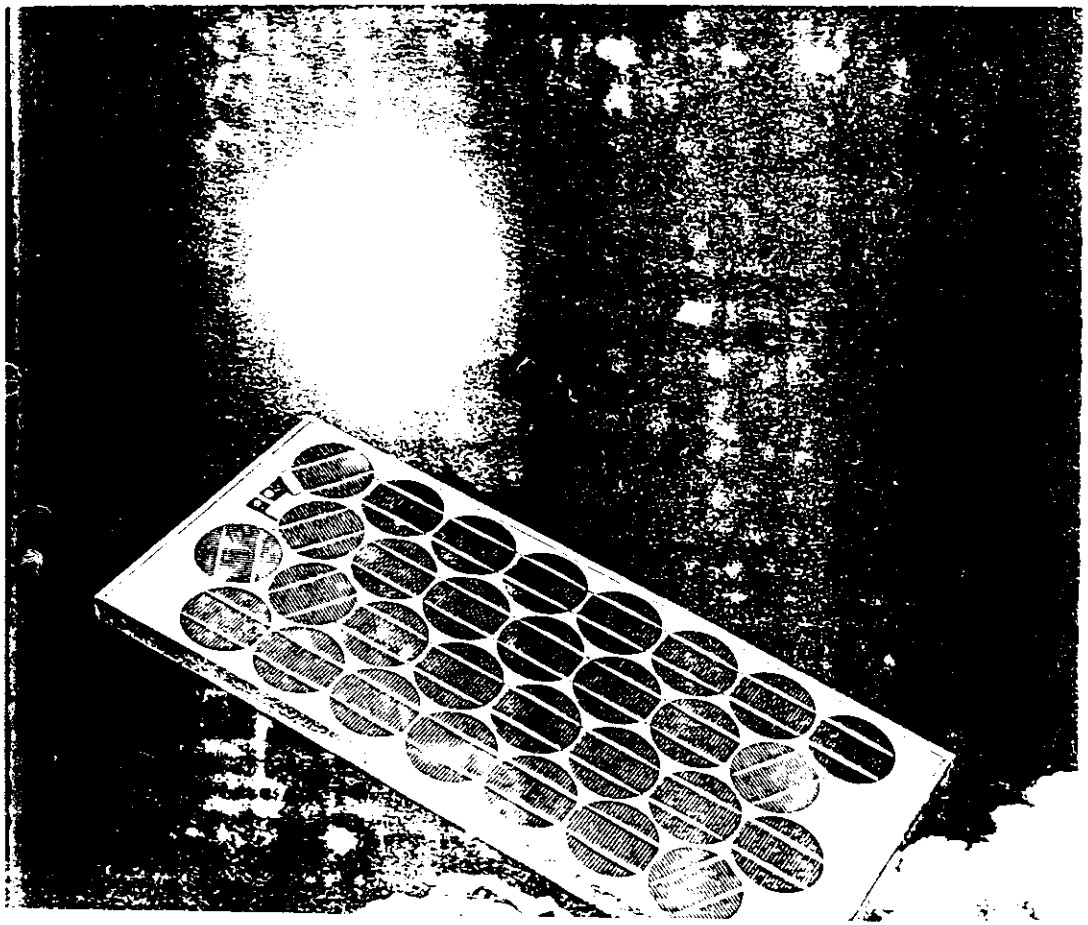

AMORPHOUS SILICON ALLOY

- **Easy to make, uses glow-discharge decomposition of silicon-containing gasses in a vacuum chamber.**

- **High absorption coefficient, needs very thin film to absorb sunlight.**

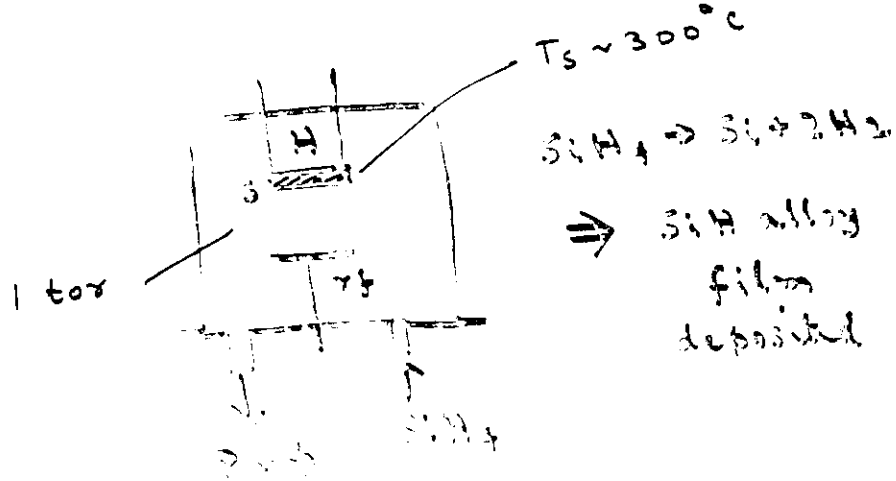

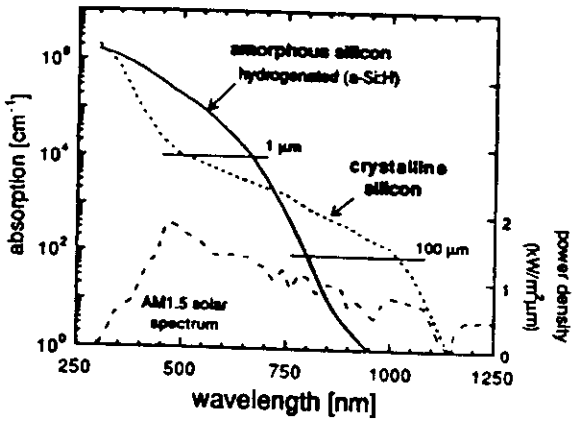

Figure 2.1: Optical absorption coefficients for hydrogenated amorphous silicon (a-Si:H) and crystalline silicon and AM1.5 (100 mW/cm² solar spectrum power density (dashed line, from [MATB4]).

5

HISTORY OF DEVELOPMENT OF AMORPHOUS SILICON

Work at STL, U.K.

- Growth of X-Si from thermal decomposition of silane.
- Use of glow-discharge process to decompose silane.
- Made silicon nitride, silicon oxide and silicon.
- Silicon was amorphous, but properties very different from conventional a-Si.
- The material showed photoconductivity, and "perhaps" doping.
- Managemnt showed no interest, project discontinued.

Work at University of Dundee, U.K.

- Interested in study of drift mobility of materials.
- Needed high resistivity material.
- Conventional a-Si not of adequate high resistivity.
- Decided to use glow-discharge a-Si and borrowed from STL the reactor.
- Carried out very systematic study and determined that the material is remarkably different. They showed that the material can be made *n*- or *p*-type.
- This, of course, led to the development of *p n* junction diodes and subsequently to solar cells.

Scope of the Talk

- Nature of disorder
- Growth of a-Si
  Role of hydrogen
- Characterization of films
  structural, optical, electrical
- degradation/metastable degradation
- Solar cells
  - different configurations
  - a-Si alloy PV design
  - single-junction
  - multi-junction
  - current status
- manufacturing issues
- problems issues
- Future trends
  - new materials

Amorphous silicon

1. No long-range order.
2. Short-range order exists, and is the same as in crystal.
3. Structural defects present.

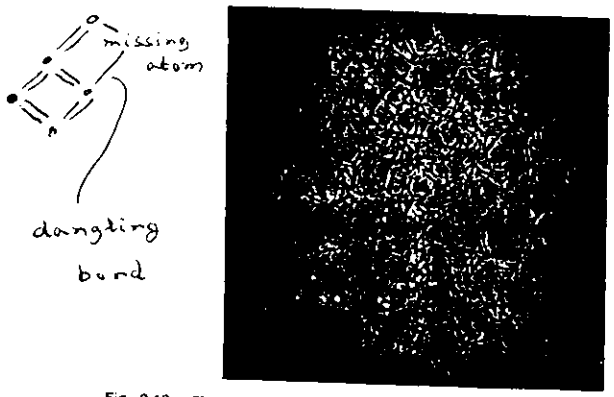

Fig. 2.12. Cluster composed of snap-together units of the type used by Polk (1971) constructing his four-coordinated continuous random network for amorphous silicon a germanium.

Figure showing lattice arrangement with structural defects.

Implication of 1. Band tails, localization and scattering.

Implication of 2. Material property similar to that in crystal.

Implication of 3. States in the gap.

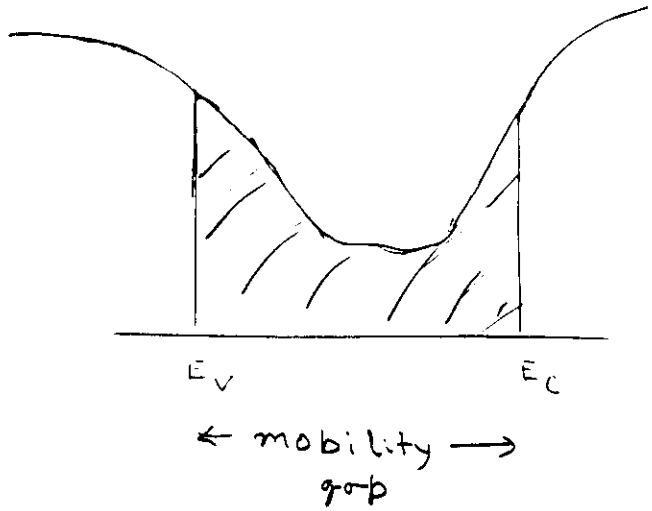

Figure showing DOS diagram

Challenge -- Sharpen band tails, reduce gap-state density.

GROWTH OF a-Si ALLOY FILM

THREE-STEP PROCESS

- GENERATION OF PLASMA
- TRANSPORT OF THE SPECIES TO THE SUBSTRATE
- GROWTH BY A PROCESS OF ADSORPTION AND SURFACE DIFFUSION

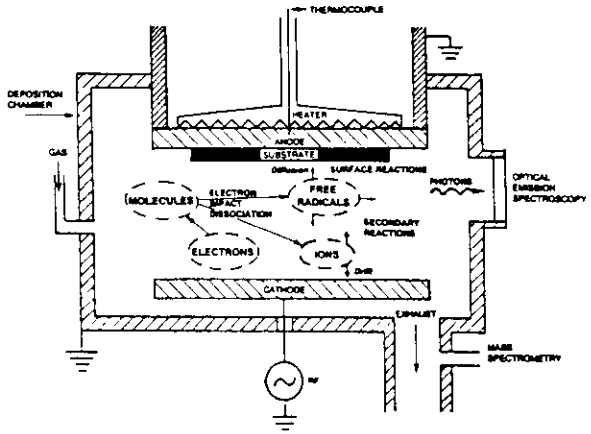

Figure 4-1 Schematic representation of the plasma-enhanced chemical vapor deposition process

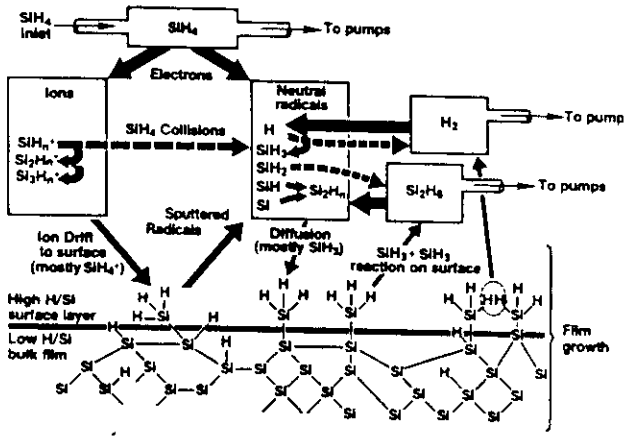

Figure 7.5-1. Model of glow discharge deposition of a-Si:H f silane [Gallagher 1987]

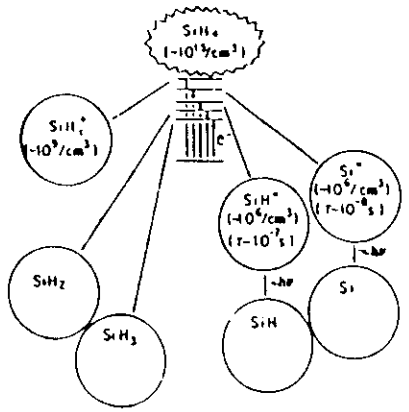

Fig. 10 Scheme of primary electron-impact process and the steady-state density of ionic and emissive species.

Table 1
Plasma diagnostic techniques used for the SiH_4 plasma

Method	Detected species
Optical emission spectroscopy (OES)	Si^*, SiH^*, H^*, H_β^*
Mass spectrometry (MS)	SiH_3^+, $Si_3H_3^+$, H^+, H_2^+
Infrared emission absorption (IR)	SiH, SiH_4
Laser-induced fluorescence (LIF)	Si, Si_2, SiH, SiH_2
Coherent anti-Stokes Raman spectroscopy (CARS)	SiH_2, SiH_4
Diode laser absorption (DLA)	SiH_3

Plasma generation

Energetic electrons in plasma generate many different species after colliding with silane

Transport of species

Many secondary reactions

Table 3
Important secondary reaction-rate constants of primarily generated radicals and parent SiH_4 molecules as well as H_2

Reaction	Rate constant (10^{-12} cm^3/s)
$Si + SiH_4 = Si_2H_4$	*
$SiH + SiH_4 = Si_2H_5$	3.3 [78]
$= Si_2H_3 + H_2$	
$SiH_2 + SiH_4 = Si_2H_6$	2.3 [83]
$SiH_3 + SiH_4 = SiH_4 + SiH_3$	-
$H + SiH_4 = H_2 + SiH_3$	[84]
$H_2 + SiH_2 = SiH_4$	0.008 [85]

GROWTH

ADSORPTION

⇒ DEPENDS ON STICKING COEFFICIENT

SURFACE DIFFUSION

⇒ DEPENDS ON DIFFUSION COEFFICIENT

CRITERION FOR GOOD QUALITY MATERIAL

LARGE SURFACE DIFFUSION SO THAT THE ADSORBED PRECURSORS CAN FIND ENERGETICALLY FAVORABLE SITES. THIS WILL RESULT IN DENSE, VOID-FREE MATERIAL.

HOW TO GET LARGE SURFACE MOBILITY

- CHOICE OF SPECIES

  SiH_2 HAS LARGE STICKING COEFFICIENT.

  SELECT SiH_3.

- ENHANCE RELAXATION

  HIGHER TEMPERATURE, LOW ENERGY ION BOMBARDMENT.

- NEUTRALIZE SURFACE

  HYDROGEN COVERAGE, ETCHING WITH FLUORINATED PRECURSORS.

ALL THESE FACTORS ARE INTERDEPENDENT.

Role of Hydrogen

10-20% hydrogen in the film.

Tying up the dangling bond.

Different bonding configuration--infrared signature.

Fig. 2.17. The set of Si—H vibrational modes for SiH, SiH_2 and SiH_3 groups, with calculated frequencies as indicated. The frequencies in brackets are estimates (Lucovsky *et al.* 1979).

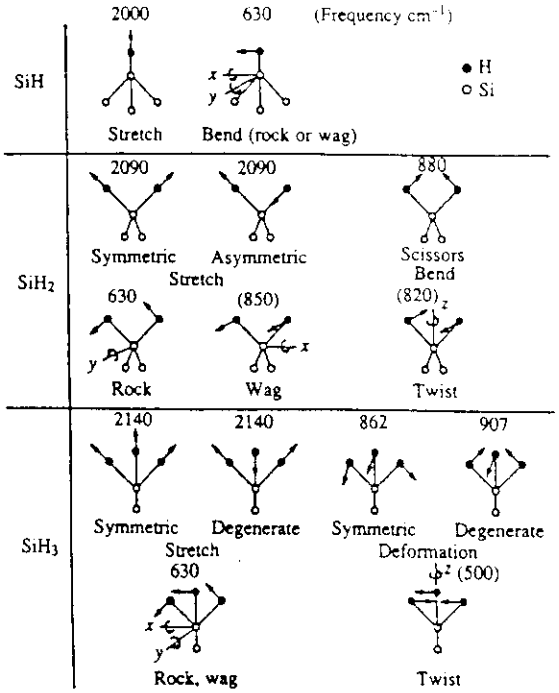

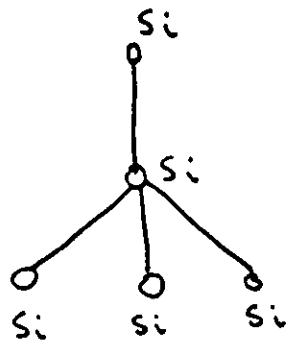

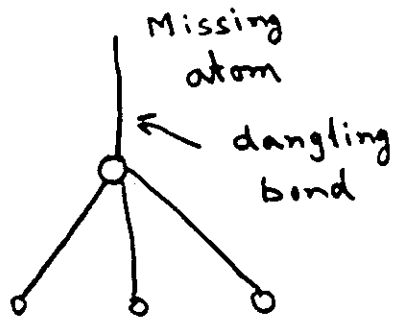

CRYSTAL

Tetrahedral Structure

Amorphous

Hydrogen ties up the dangling bond

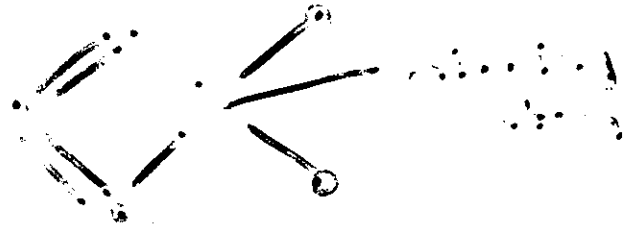

Creation of dangling bonds

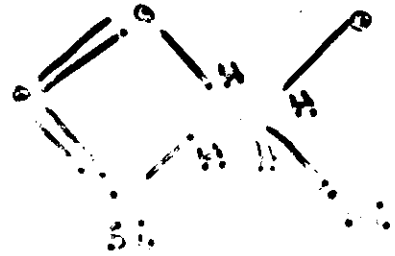

Characterization of a-Si alloy

Structure

Hydrogen content

Optical absorption

Electrical conductivity

Photoconductivity

Measurement of defect state density

Structure

X-ray, TEM

Broad halo

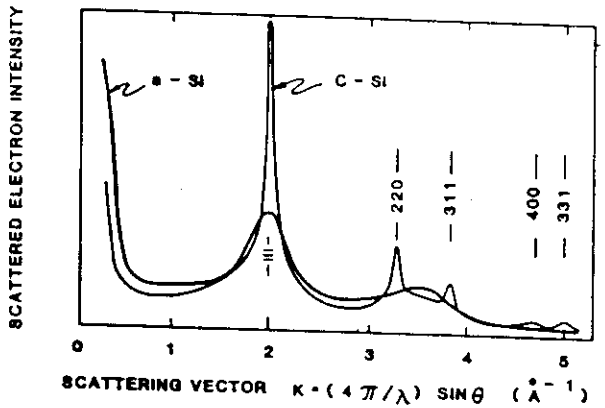

Fig. 2.13. Electron diffraction pattern (Moss and Graczyk, 1969) of amorphous silicon and of the same film after partial crystallization.

DETERMINATION OF HYDROGEN-CONTENT

Infra-red absorption

Hydrogen effusion

Fig. 2.16. Examples of the IR transmission spectra for a-Si:H samples deposited at different growth conditions. The deposition power is indicated; A and C refer to deposition on the anode and cathode (Lucovsky *et al.* 1979).

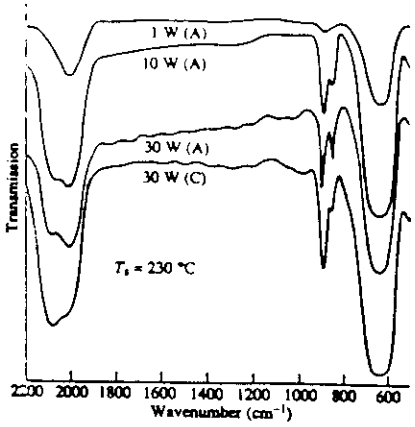

Fig. 2.24. Temperature dependence of the rate of hydrogen evolution i material deposited under different conditions: (*a*) low power CVD grov (*b*) PVD columnar material; (*c*) deposited at room temperature and wit high hydrogen content (Biegelsen *et al.* 1979).

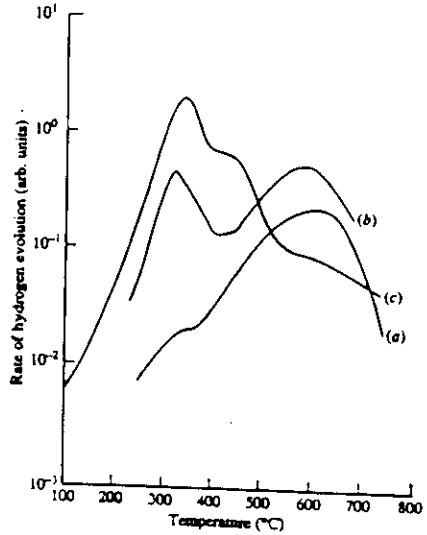

Optical Absorption

Band to Band transition

Crystals

Direct bandgap GaAs

Indirect bandgap Si

Direct

(high absorption)

Indirect

Transition involves phonon to conserve momentum (low absorption)

Direct gap

$$\alpha h\nu = A (h\nu - E_g)^{1/2}$$

Indirect gap

$$\alpha h\nu = B (h\nu - E_g \pm E_{ph})^2$$

Amorphous semiconductors

Selection rule is not pertinent

Non-direct bandgap

High absorption

Tauc et al

Assumes parabolic ~~bandgap~~ band edge, constant matrix element for transition

$$(\alpha h\nu)^{1/2} = A (h\nu - E_o)$$

$E_o \rightarrow$ optical gap

Note: mobility gap is tighter than optical gap measured from Tauc plot.

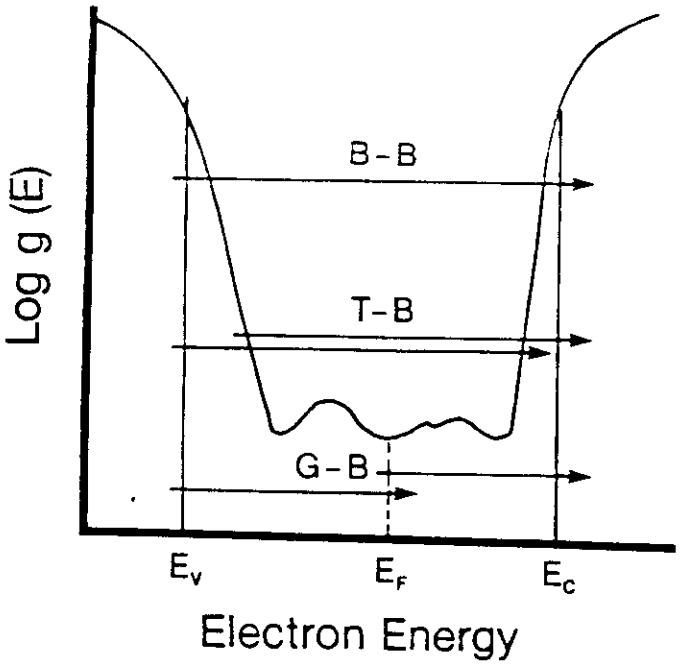

URBACH EDGE

Transition from localized band tail to extended states

$$\alpha(h\gamma) = \alpha_o \exp [(E-h\gamma)/E_u]$$

Below the fundamental absorption, one finds exponential absorption with a characteristic energy ~50-100 mV. Valence band tail is usually less steep than the conduction band tail; the transitions are therefore mostly from valence band tail.

E_u is therefore a measure of valence band tail slope.

Three regions of absorption

i) fundamental band-to-band absorption
ii) absorption due to tail states
iii) absorption due to defect states deep in the gap

Variety of techniques for probing the different regions

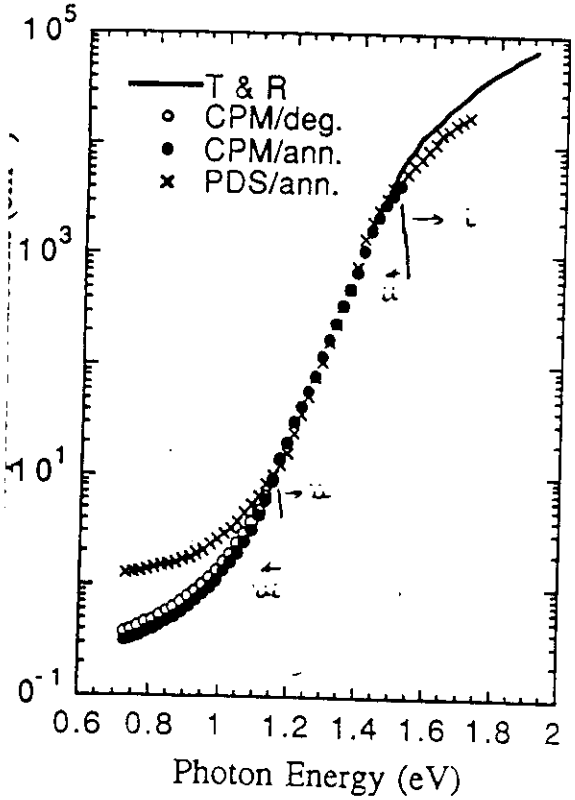

Dark conductivity

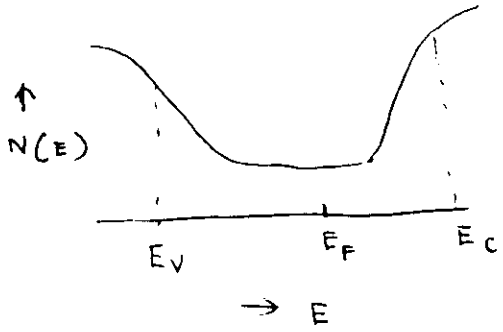

$$\sigma = \sigma_0 \exp\left[-(E_C - E_F)/kT\right]$$

At high temperature, one usually obtains a linear plot of $\ln\sigma$ vs $1/T$ which gives a measure of Fermi level position.

Note: E_F, E_C and also the bandgap depend on temperature so the situation is more complicated.

At lower temperature, conduction takes place by hopping at the band tails or at the Fermi level where the states are localised

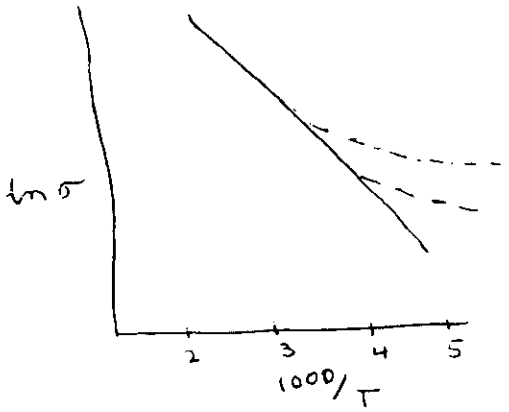

As the defect density increases, there is more departure from the linear plot.

Photoconductivity

$$\sigma_{ph} = n e \mu_n + p e \mu_p$$

$$\equiv n e \mu_n \quad \text{since } \mu_n \gg \mu_p$$

$$= G e [\mu\tau]_n$$

$G \rightarrow$ optical excitation rate

$$= n/\tau$$

σ_{ph} gives you an indication of $\mu\tau$ for electrons.

$\mu\tau$ is determined by recombination process for the excess carriers and depends on the total number of recombination centers

Complex problem

- charged defects
- neutral defects
- capture cross section
- Fermi level dependence

Example of dependence of σ_{ph} on Fermi level position

$\mu\tau|_n$ increases as E_f moves closer to E_c

$\mu\tau|_p$ decreases

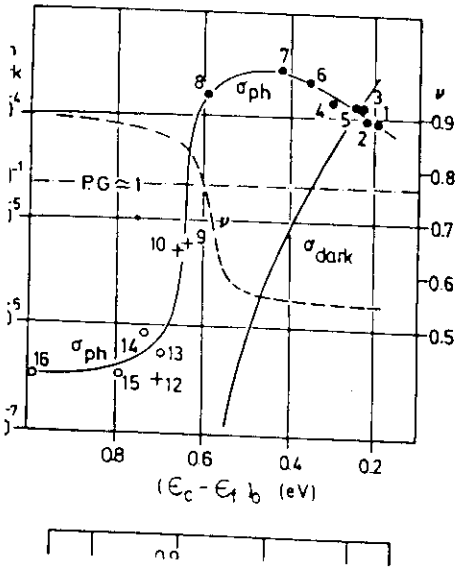

Fig. 9.20. Photoconductivity at 295 K plotted against $(\varepsilon_c - \varepsilon_f)_0$, the position of the dark Fermi level for phosphorus-doped (●), undoped (+), and boron-doped (○) specimens. The broken line represents the exponent ν (see right-hand ordinate) in the intensity dependence $\sigma_{ph} \alpha I^{\nu}$. σ_{dark} is a typical dark-conductivity curve. P.G. $\simeq 1$ refers to unit photoconductive gain at a field of 3×10^3 V cm^{-1} [9.10]

MEASUREMENT OF DEFECT DENSITY

- Photoconductivity
- Sub-bandgap absorption
- Electron spin resonance

A variety of techniques which use device configuration like Schottky and *p i n* structure

Table 2.2-1 Typical Room Temperature Characteristics of Device-Quality, Undoped a-Si:H

Property	Typical Values	Units
optical bandgap, E_g	1.7 to 1.8	eV
hydrogen content, C_H	8 to 15	at.%
refraction index, n, at 600 nm	~ 4.3	
electron drift mobility, μ_e	≥ 1	$cm^2V^{-1}s^{-1}$
hole drift mobility, μ_h	≥0.008	$cm^2V^{-1}s^{-1}$
electron lifetime, τ_e	≥ 2×10^{-7}	s
hole lifetime, τ_h	≥ 10^{-6}	s
$\mu\tau$ (electron)	≥ 2×10^{-7}	cm^2V^{-1}
$\mu\tau$ (hole)	≥ 10^{-8}	cm^2V^{-1}
hole diffusion length, L_h	0.3	μm
AM1 photoconductivity, σ_l	5×10^{-5} to 10^{-4}	S/cm
dark conductivity, σ_d	10^{-11} to 10^{-10}	S/cm
σ_d activation energy, E_a	0.7 to 0.9	eV
AM1 photosensitivity, σ_l/σ_d	≥ 1×10^6	
valence band tail slope, E_v	42 to 50	meV
conduction band tail slope	~ 25	meV
ESR spin density	7×10^{14} to 10^{16}	$eV^{-1}cm^{-3}$
density of states at E_f	5×10^{14}	$eV^{-1}cm^{-3}$
SiH_2/SiH	~ 0	
microvoids (d > a few Å)	~ 0	
intrinsic stresses	≤ 400	MPa

LIGHT-INDUCED EFFECTS IN a-Si ALLOY

First observed by Staebler and Wronski in 1977

1. **Exposure to AM1 light for 2 h reduces the dark conductivity by several orders of magnitude.**

2. **Photoconductivity also reduces by a factor of 3 to 5.**

   The effect is reversible.

   Original values are restored by annealing at ~150 °C.

   Later work showed similar changes in

- **e s r**
- **photoluminescence**
- **sub-bandgap absorption**
- **diffusion length**
- **solar cell performance**

Note: Degradation does not continue indefinitely -- it saturates.

>ark conductivity

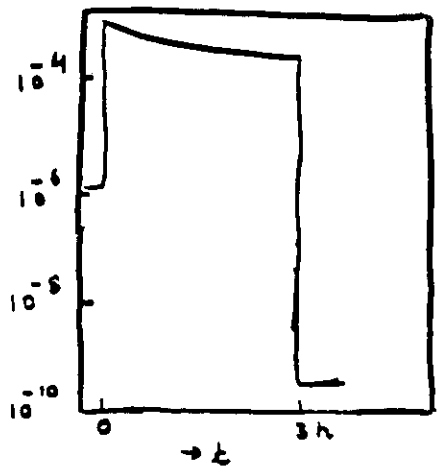

σ_d decreased by 4 orders of magnitude.

Other groups — large dispersions. Some results show large change in σ_d; others show very small change. actual change depends on F.L. position

Surface vs bulk effects.

What determines σ_d.

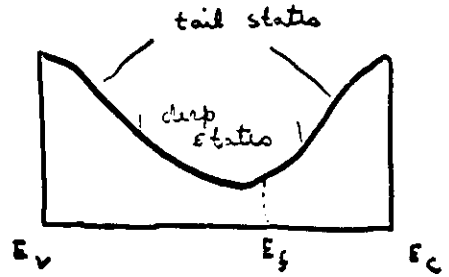

Tail states
- due to disorder (CFO model)

Deep states
- due to defects

Position of E_f governed by gap state distribution.

It is possible to create new states in the gap without shifting E_f i.e without any change in σ_d.

What do we learn from σ_d measurements.

1. Perhaps new states in the gap are created since E_f moves
2. Since in p-type material, E_f moves upward whereas in n-type material E_f moves downward, states are created both above and below mid-gap.
3. Absence of changes in σ_d is not a sufficient criterion to indicate that light induced effects do not take place.

Photoconductivity

σ_{ph} is governed by recombination kinetic

$\sigma_{ph} \propto \mu\tau$ $\mu \rightarrow$ mobility

$\tau \rightarrow$ life time

$\tau \propto \frac{1}{N_r}$ $N_r \rightarrow$ No of recombination centres

Light exposure reduces σ_{ph},

i.e τ decreases $\rightarrow$ N_r increases

$\rightarrow$ new states are created in the gap.

Caution

1. If N_r is large to start with, one may not see any change in σ_{ph}
2. Photoconductivity $\rightarrow$ complex process. σ_{ph} depends on F.L. position, capture cross section etc.

VARIETY OF MEASUREMENT TOOLS

- Defects are created both below and above Fermi level.
- Impurities like O, N, C present in large quantities >10^{19} cm^{-3} increase the degradation; the consensus, however, is that it is an intrinsic problem.

Effect of light soaking on Spine

A state $N_s \sim 9.10^{15}\ cm^{-3}$

B state $N_s \sim 1.8.10^{16}\ cm^{-3}$

Similar annealing behaviour.

How can the bonds be broken?

How much energy is involved?

Actual energy < light energy (~2 eV)

Role of Recombination

pin diodes degrade on light soaking

very similar degradation on appl^{n} of forward bias in dark.

What is common → trapping and recombination

Importance of recomb^{n}

→ less degradation if diode is kept reverse biased during illumination

Results on Schottky diode

In a pin diode

dark f b → both trapping & recomb^{n}

In a Schottky diode

→ negligible minority carrier injection

→ no recombination

→ only trapping

Absence of degradation in SBD under f.b. will prove that trapping alone is not adequate to cause degradation.

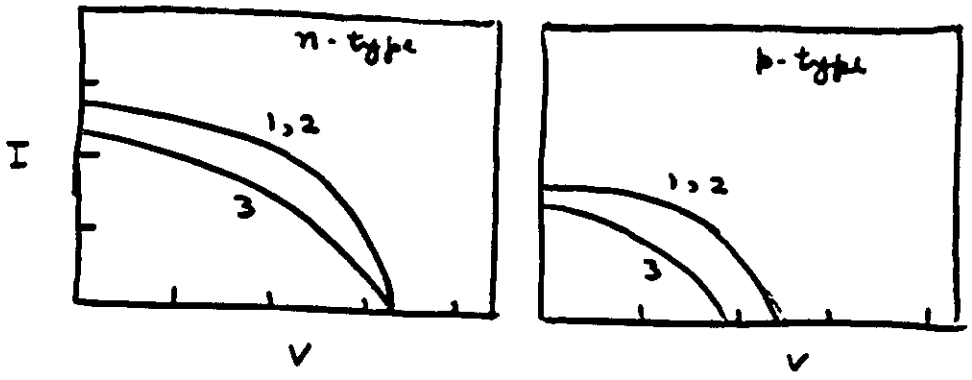

1 → A state

2 → dark f b soaking

3 → light soaking

Possible mechanism

- Recombination releases energy to break weak / strained bond
- To prevent the neighboring bonds from recombining, H-bond switching takes place.

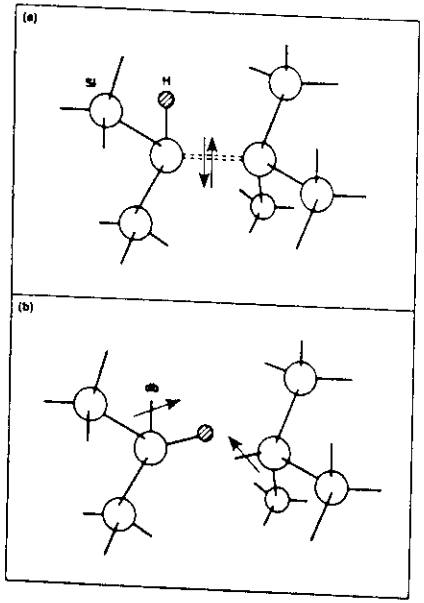

Figure 2.6.1-3 A possible microscopic process leading to the creation of metastable dangling bonds [Stutzmann et al. 1985].

Many controversies – several kinds of light-induced defects.
We still do not understand the mechanism

Is there an upper limit to generation of new defects?

Yes

1. Total number of weak bonds is finite
2. As the defects are created, thermal annealing brings them back to original configuration also.

   ⇒ saturation in defect degradation

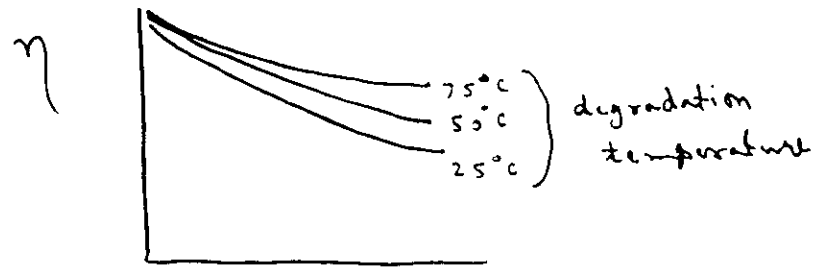

Junction device under illumination

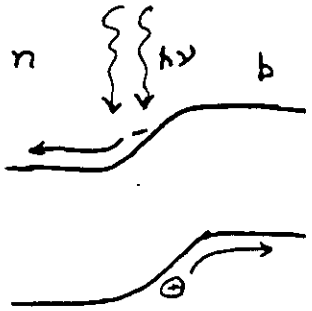

Shine light

$h\nu > E_g$

Electron and hole pairs are created and separated by electric field. A voltage develops → p positive.

Current flows in opposite direction to forward bias current.

$$I = I_s \left[\exp\left(\frac{qV}{kT}\right) - 1 \right] - I_L$$

Lighted I V characteristic

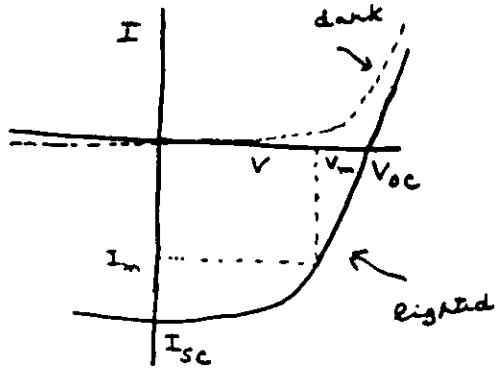

At open circuit $I = 0$

$$V_{oc} = \frac{kT}{q} \ln\left(\frac{I_L}{I_s}\right)$$

Maximum power point at V_m, I_m

Define fill factor (F.F)

$$F.F. = \frac{V_m I_m}{V_{oc} I_{sc}}$$

$$\text{Efficiency} = \frac{(V_{oc})(I_{sc})(F.F)}{P_{in}}$$

F.F. depends on 1) carrier collection efficiency
→ recombination

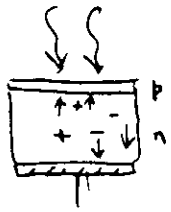

2) Series resistance R_s
Slope at $I = 0$
→ bulk, contacts

3) Shunt resistance
Slope at $V = 0$
→ leakage

Optimization of efficiency

Efficiency depends on photon collection

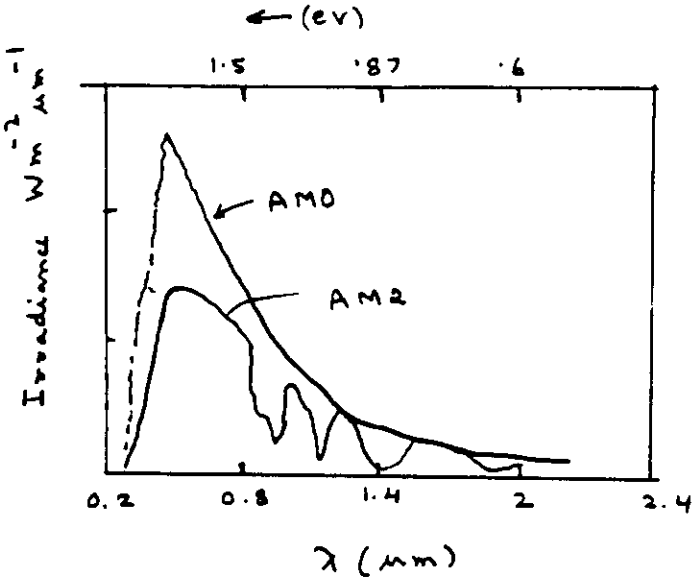

SOLAR SPECTRUM

AM0 → outside atmosphere

AM1 → Sea level sun at zenith

AM2 → Sea level sun 60° from zenith

Absorption spectrum

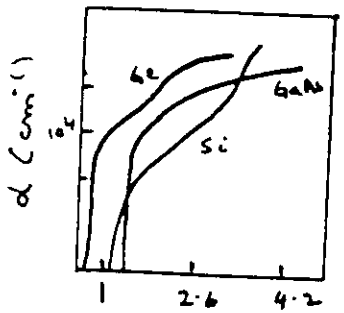

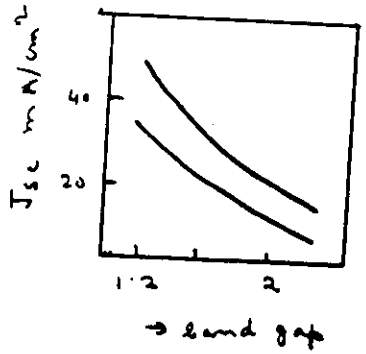

J_{sc} consideration

As E_g increases, J_{sc} decreases.

∴ should use small E_g so that all the photons may be absorbed.

V_{oc} consideration

$V_{oc} \propto \ln \frac{J_{sc}}{J_s}$

$J_s \propto \exp - \frac{E_g}{2kT}$

E_g increases, V_{oc} increases

∴ should use large E_g to maximize V_{oc}

Optimum efficiency as a function of band gap

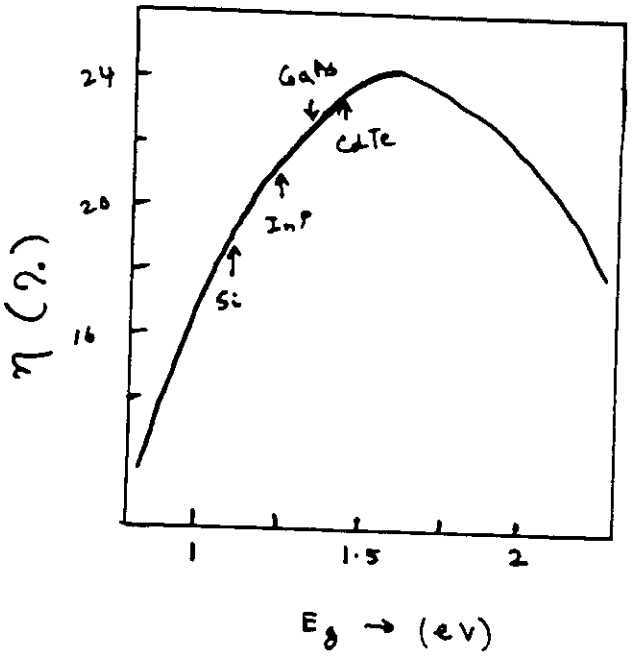

Material requirement

→ optimum gap

→ good life time

→ high absorption

Device structures

1) pn junction

2) pin

3) metal - semiconductor (m s)

4) metal - insulator - semiconductor (m i s)

5) Tandem or stacked structure

6) Heterostructures

p-n junction

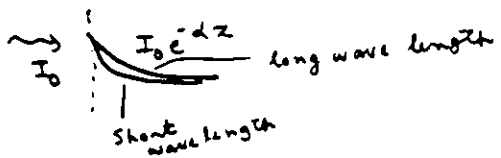

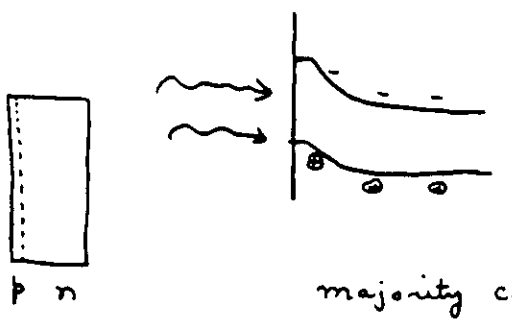

majority carrier life time

minority carrier life time
(diffusion length)

bulk recombination

surface recombination

One can also have n p

and p i n solar cells

metal - semiconductor contacts
(Schottky diode)

Instead of a p-n junction, one can also create a barrier by putting a thin metal on top of a semiconductor

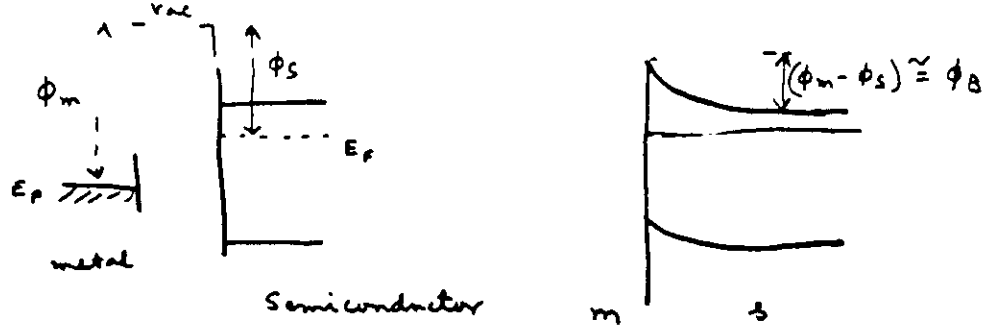

Adv : Easy to make

Low temp. process

Disadv: low V_{oc}

Remember $V_{oc} \propto \ln \frac{J_{sc}}{J_0}$

For Schottky diode

$J_0 \propto \exp - \frac{\phi_B}{kT}$

ϕ_B is small, J_0 is large

$\therefore V_{oc}$ is small

I S device

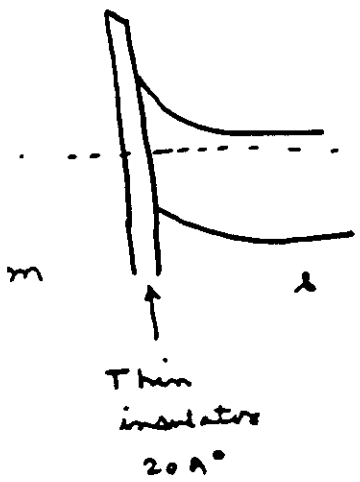

If you put a thin insulator between metal and semiconductor,

J_s decreases

Two reasons:

1) ϕ_B may increase because of charge in the oxide

2) electrons now have to tunnel thro' oxide

$J_s \propto \exp\left(-\frac{\phi_B'}{kT}\right) \exp(-\delta$

δ = oxide thickness

δ should be thin, otherwise J_{sc} will go down too.

Adv. Ease of fabrication

Large V_{oc}

Disadv: Uniform thin oxide is difficult to attain over large area

Tandem structures

Use two cells with different band gaps stacked one on top of other.

This will allow you to catch photons over a wider energy range.

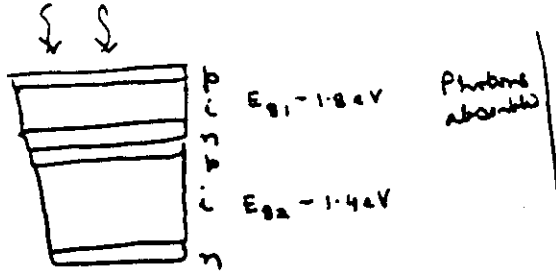

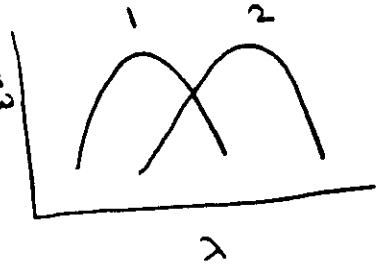

note: you have to choose the thickness of the layers such that the individual currents match.

Heterostructure

Homojunction → when a junction is made by using the same semiconductor with different doping levels

Heterojunction → junction is made between two different semiconductors.

The tandem structures are heterostructures.

Other examples

p GaAlAs - p GaAs - n GaAs structure

Wide gap window to reduce surface recombination

Cu_xS - CdS cells

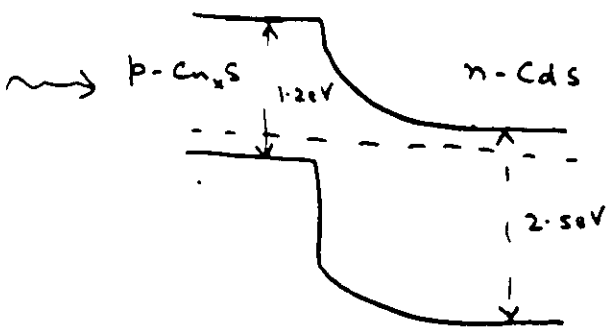

CdS - $CuInSe_2$ cells

2.4 eV CdS

1.02eV $CuInSe_2$

morphous Silicon Alloy Solar Cell

p i n structure is most common

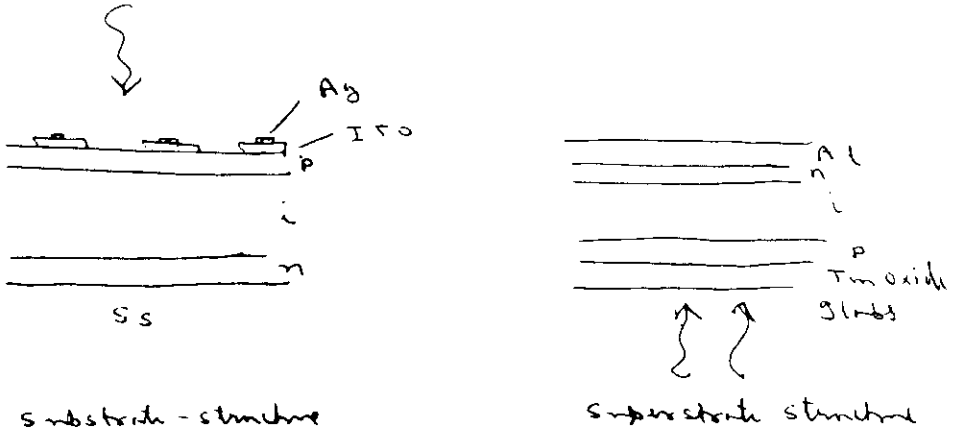

substrate - structure

superstrate structure

Light enters through the p-side so that holes do not have to move far (Note: $\mu\tau$ for holes is low)

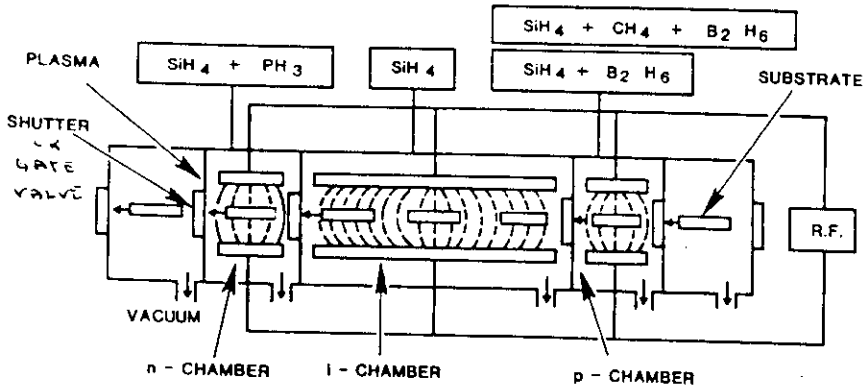

Fig. 3.49. Consecutive, separated reaction chamber apparatus for fabrication of a-Si : H films (Kuwano *et al.*, 1981).

DESIGN CONSIDERATIONS

Thickness of *i* layer

J_{sc} should increase with thickness
FF would go down
V_{oc} should be relatively insensitive

Peak efficiency would be at an optimum thickness of *i* layer

Theoretical calculation assuming 60% reflection at the back contact

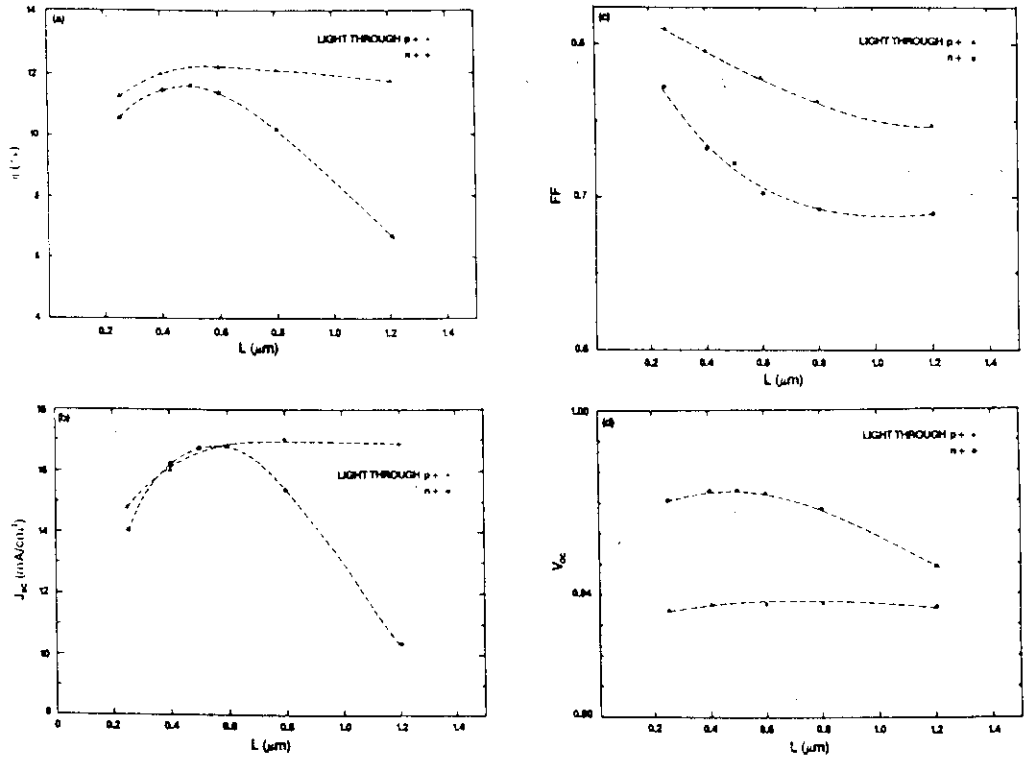

FIG. 32. Computed values of (a) efficiency, (b) short-circuit current, (c) fill factor, (d) open-circuit voltage as a function of intrinsic layer thickness for parameters given in Table I.

Note that it is desirable to have light incident thro' p-layer.

PROBLEM OF LIGHT-INDUCED DEGRADATION

Since $\mu\tau$ decreases after light soaking, cell efficiency will go down. The problem is more in cells with higher thickness since the carriers have to move far.

Less degradation in thinner cells, but the initial efficiency is also lower.

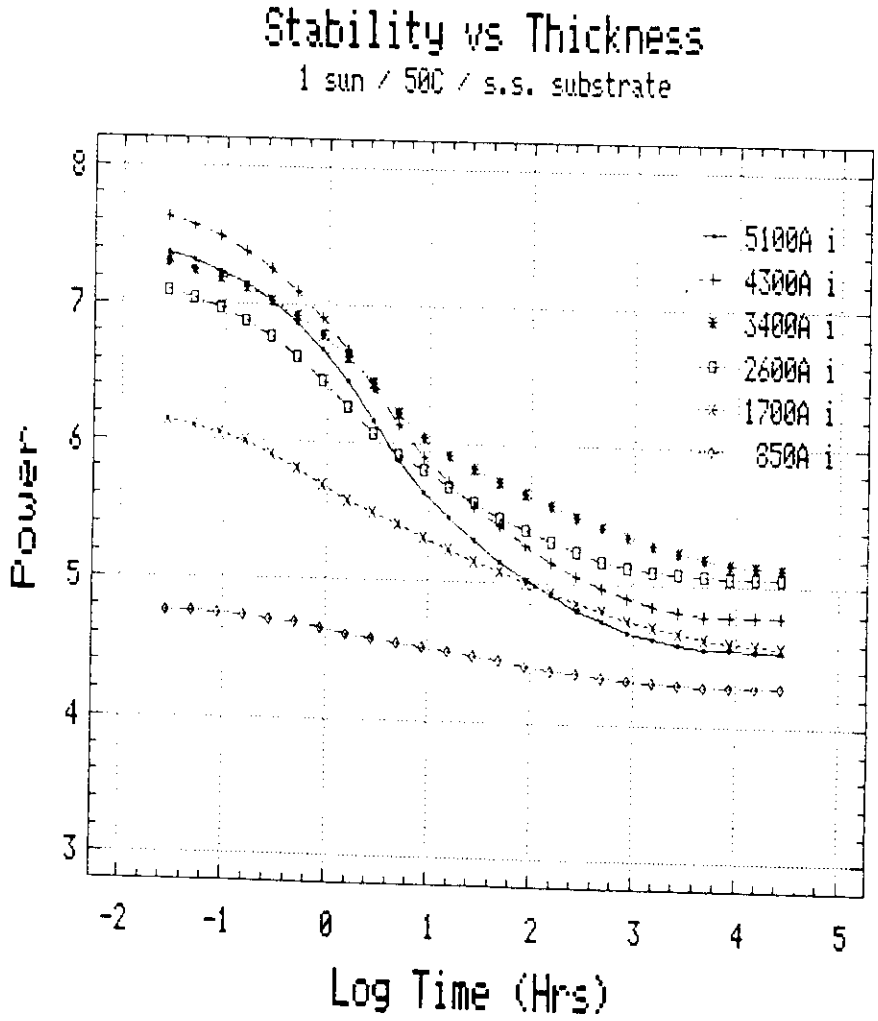

Fig. 33. Extrapolated power versus time for various thicknesses of a-Si:H single-junction cells, deposited on bare stainless steel substrates, for one sun and 50°C conditions.

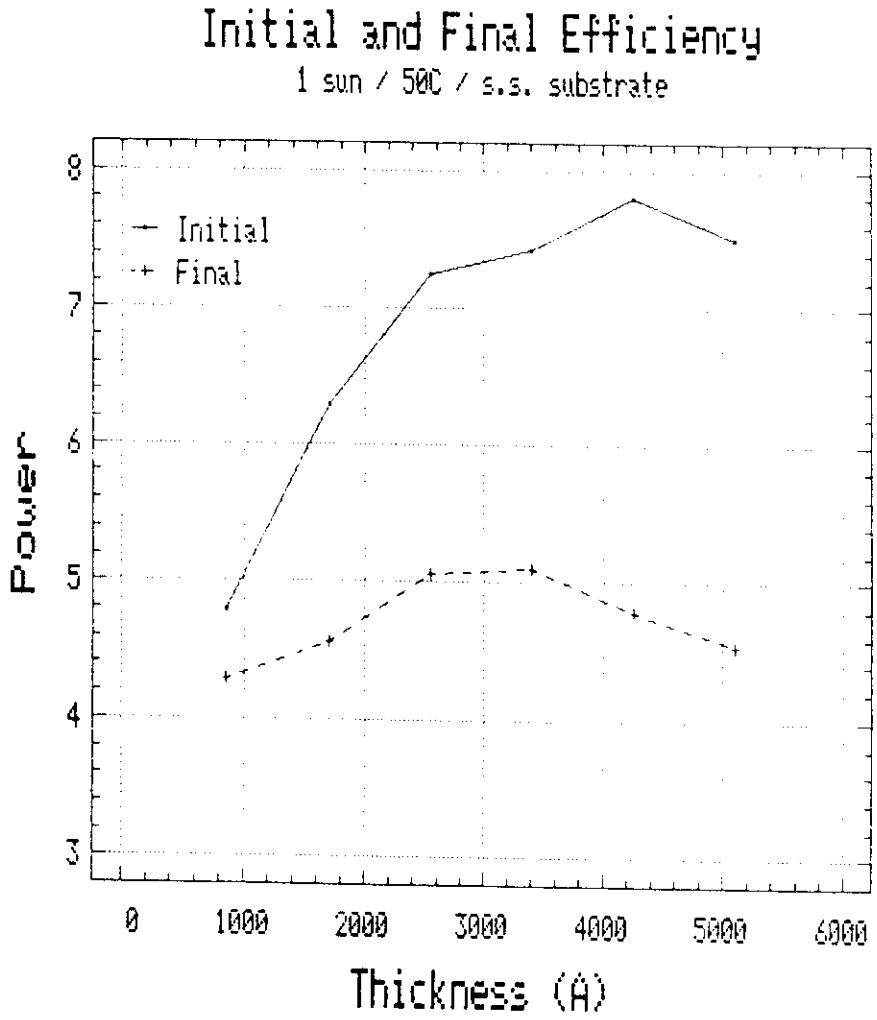

Fib. 34. Initial and final efficiencies for the extrapolated one sun data shown in Fig. 33.

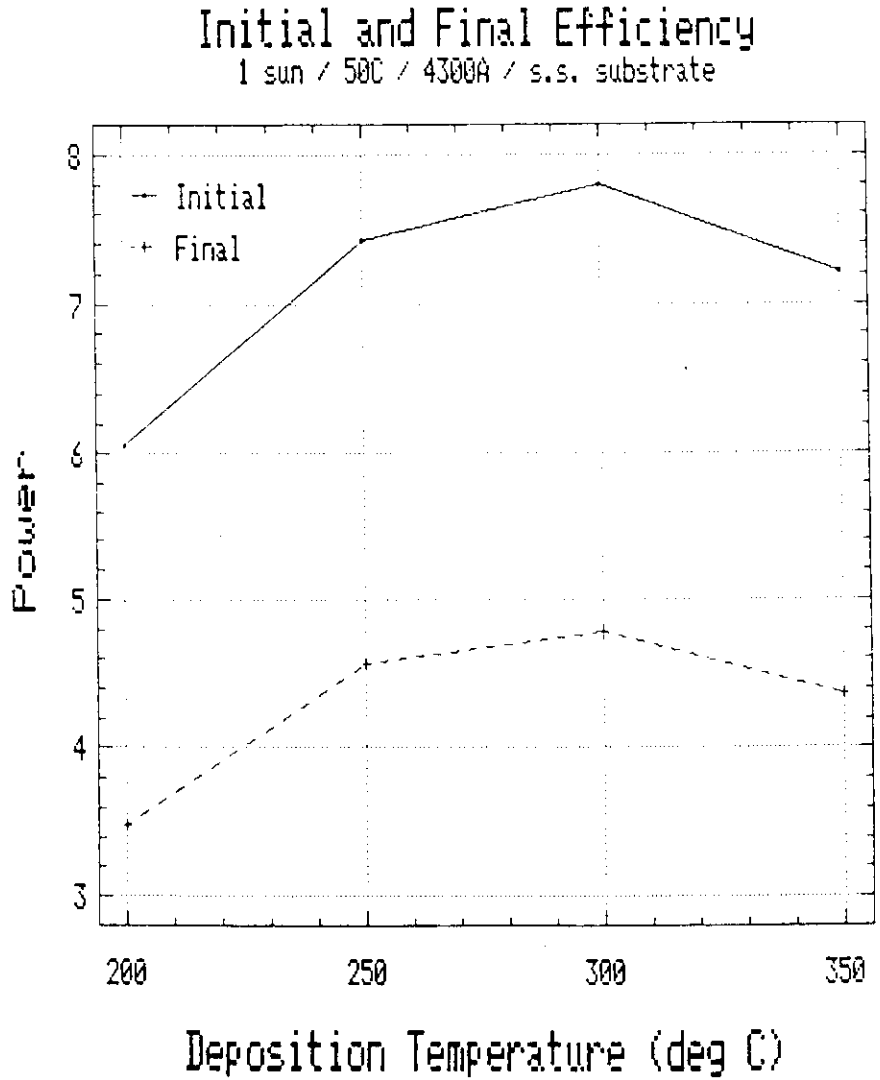

Fig. 37. Initial and final efficiencies for the extrapolated one sun data of a-Si:H single-junction cells, deposited at various temperatures at a thickness of 4000 angstroms.

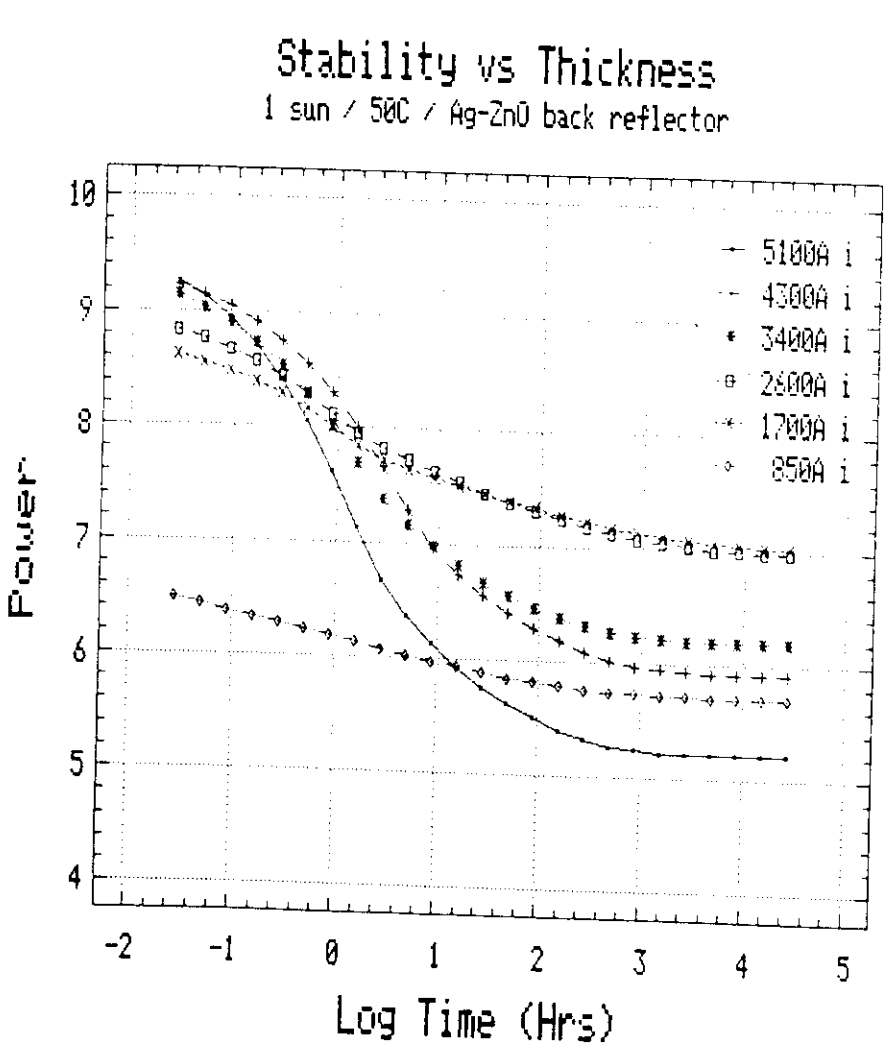

Fig. 35. Extrapolated power versus time for various thicknesses of a-Si:H single-junction cells, deposited on specular Ag/ZnO back reflectors, for one sun and 50°C.

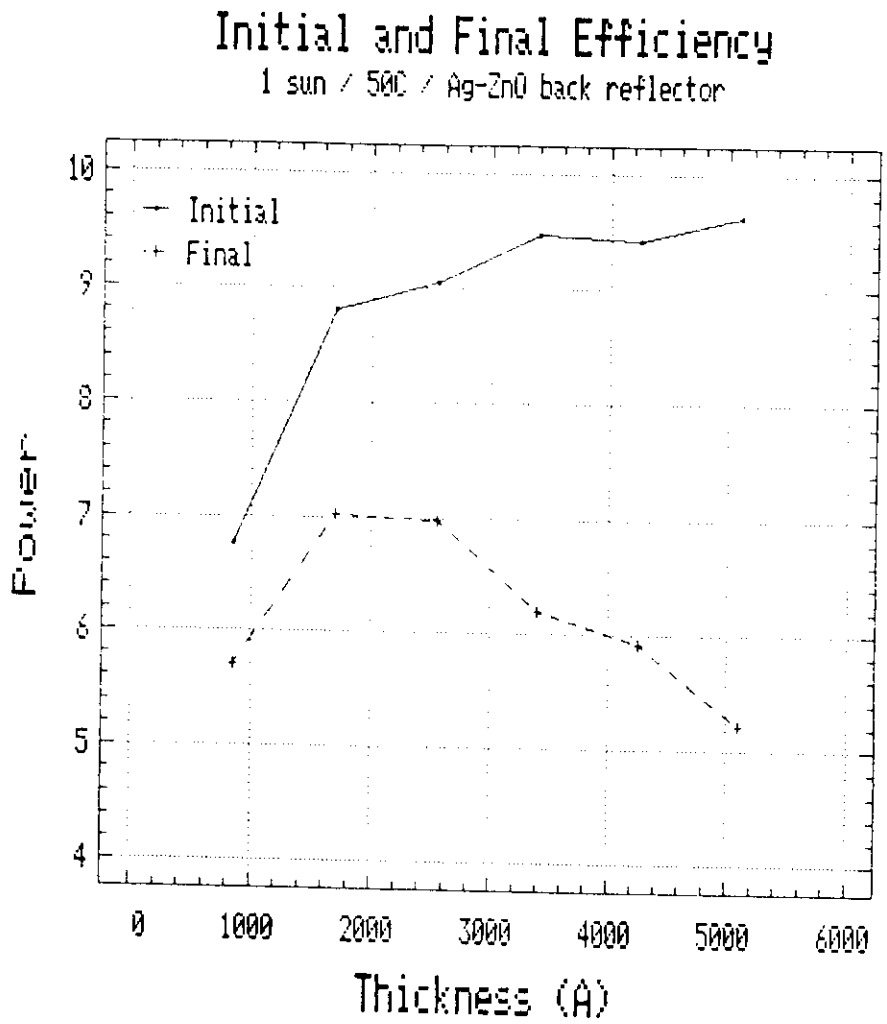

Fig. 36. Initial and final efficiencies for the extrapolated one sun data shown in Fig. 35.

dependence of η on dep. rate

Table 2. **Material Properties and Cell Performance for Samples Prepared at Two Different Deposition Rates.**

Deposition rate	0.14 nm/sec	1.35 nm/sec
Void fraction	1%	4%
Predominant void diameter	·	0.9 nm
Hydrogen content	8%	12%
Microstructure fraction (R)	8.4%	18.4%
C_H (2000)	6.4%	6.3%
Initial efficiency	7.85%	6.31%
Degraded efficiency	6.53%	3.5%
Initial red fill factor	0.67	0.52
Degraded red fill factor	0.52	0.43
Initial blue fill factor	0.73	0.67
Degraded blue fill factor	0.67	0.40

CELL STRUCTURE AND MATERIAL

- Simplest Cell Structure — Single p-i-n

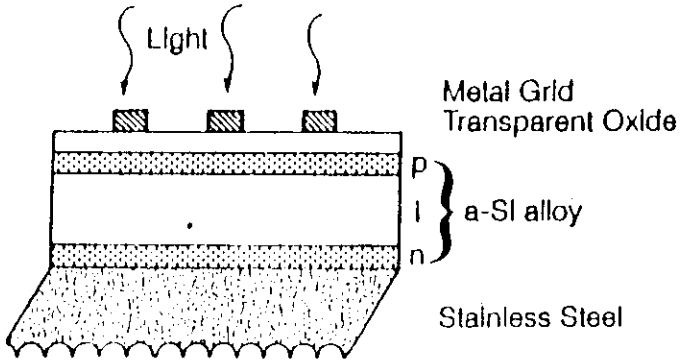

- To obtain high efficiency, you must capture all the solar photons
- Therefore, you must make i-layer thick

PROBLEMS WITH SINGLE CELL STRUCTURE

- Theoretical maximum efficiency is low (~ 13%).
- Efficiency decreases after exposure to light.

LIGHT-INDUCED DEGRADATION

- EXPOSURE TO LIGHT CREATES NEW DEFECTS IN THE MATERIAL.
- THESE DEFECTS HAVE AN ADVERSE EFFECT ON CARRIER TRANSPORT AND, AS A RESULT, EFFICIENCY DECREASES ON LIGHT EXPOSURE.
- THERE IS A SIMULTANEOUS DEFECT ANNEALING PROCESS SO THAT AFTER A FEW HUNDRED HOURS, THE EFFICIENCY STABILIZES AT A NEW VALUE.
- THE PROBLEM IS LARGER IN SINGLE-CELL STRUCTURE WHERE ONE USES THICKER LAYERS TO CAPTURE THE PHOTONS AND, THEREBY, TO OBTAIN HIGH INITIAL EFFICIENCY.

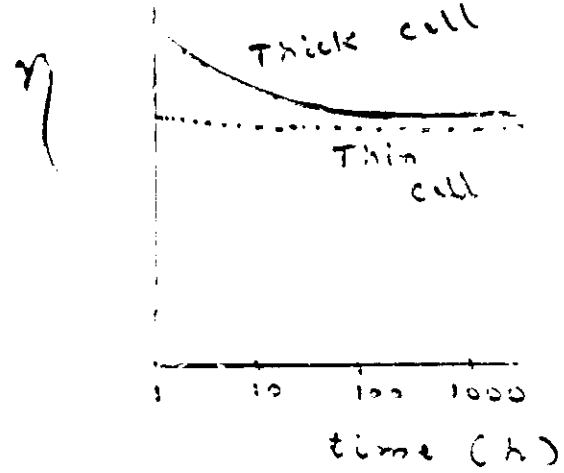

TANDEM CELL APPROACH

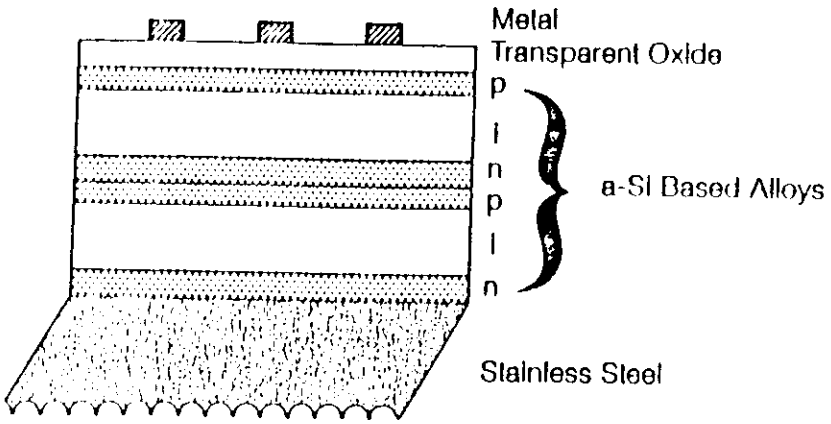

ADVANTAGES OF TANDEM CELLS

1. You can use different band gap material for the different I-layers thereby obtaining more efficient photon collection.
2. Since the top layer is thin and the bottom layer does not receive as much light, the cells are inherently more stable.

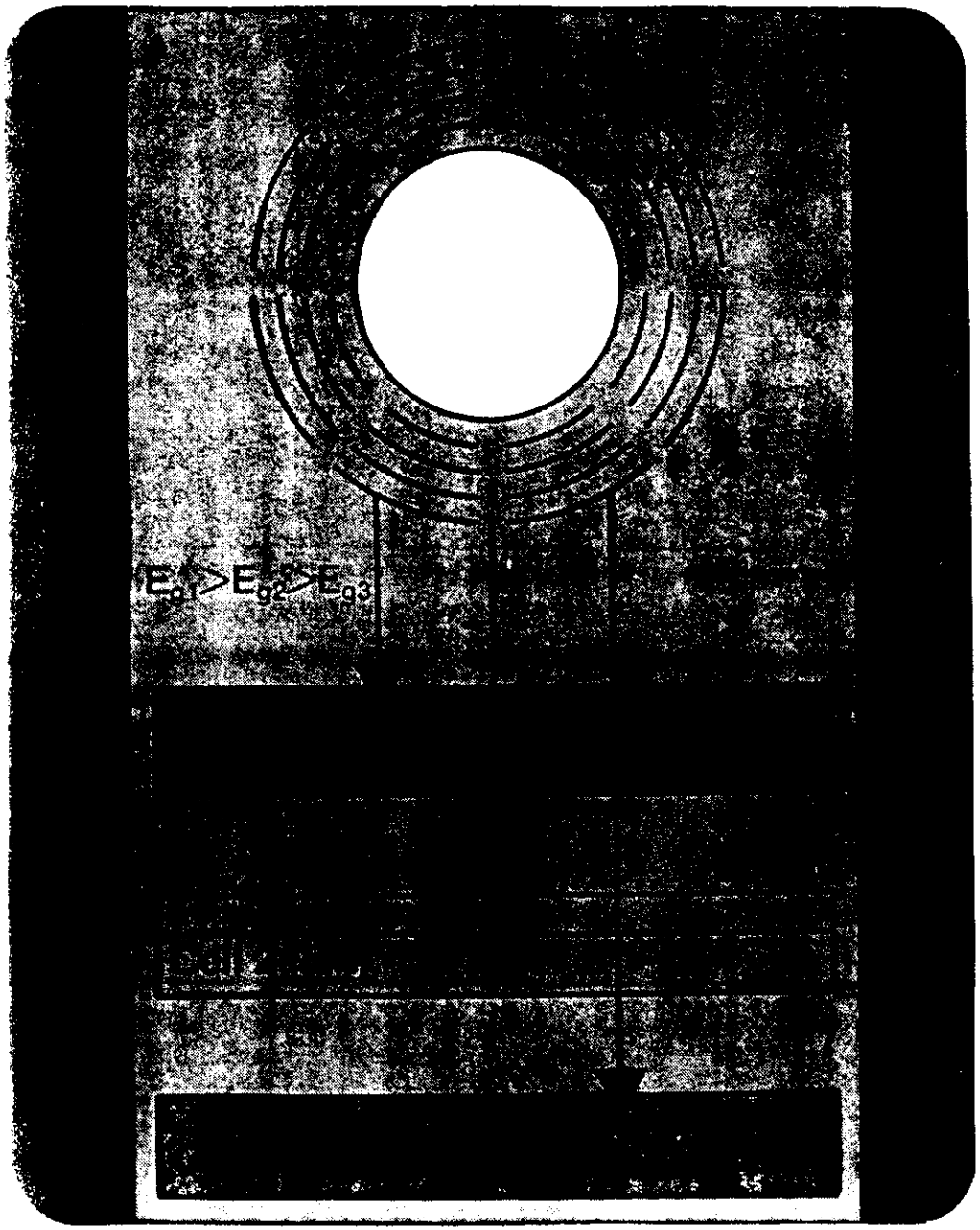

USSC R&D TRIPLE-CELL STRUCTURE

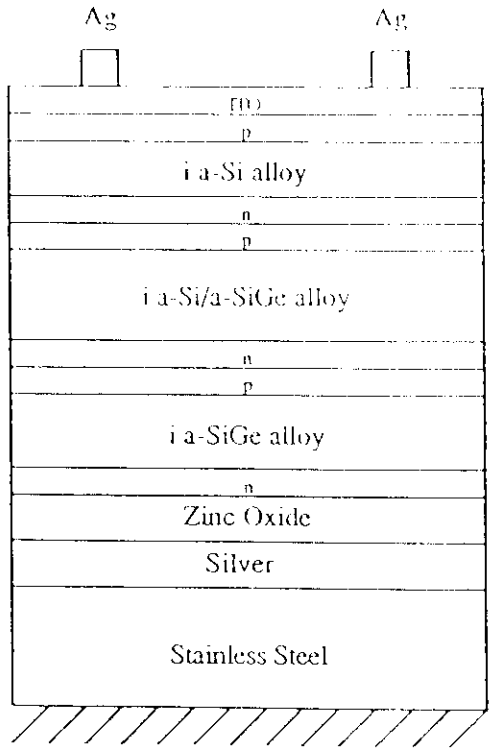

Multijunction Solar Cell

Theory

Stack of infinite number of cell

Efficiency — 60%.

from thermodynamic calculations

Practical limit based on triple stacked amorphous solar cell

Efficiency - 20 to 30%.

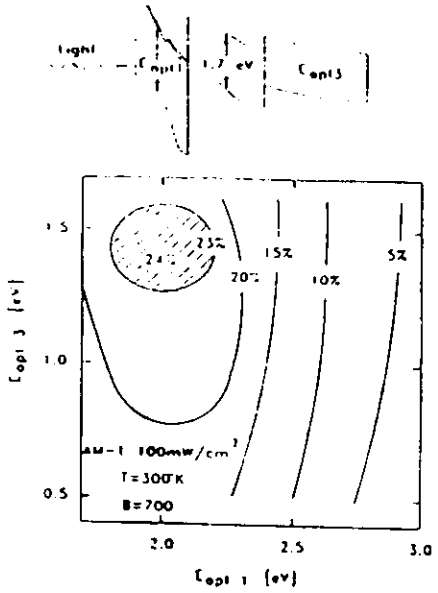

Figure 2.25 Theoretical conversion efficiency of a two-terminal, triple junction cells with a 1.7 band-gap middle junction cell. The optimum conversion efficiency of 24% is obtained from E_{g1} = 2.0 eV and E_{g3} = 1.45 eV.

CELL EFFICIENCY

Multijunction, multi-bandgap approach

Requirements for high efficiency with good stability

- **High quality back reflector**
- **High efficiency component cells**
- **High quality doped layers**
- **High quality "tunnel" junction**
- **Optimum matching of the component cells**

CONSIDERATIONS FOR BACK REFLECTOR

Requirements

- **High reflectivity**
- **Good texture to scatter light at an angle larger than the critical angle**

OPTICAL ENHANCEMENT

- Multiple Internal Reflection
- Enhancement in Red Response
- Increase in Short Circuit Current

BACK REFLECTOR

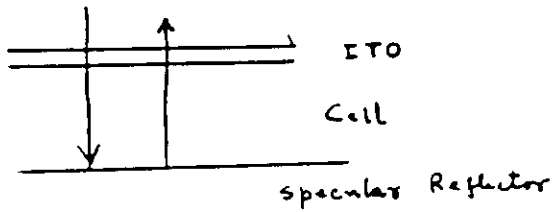

2 passes

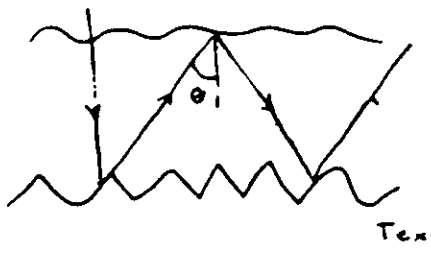

Multiple passes

MULTIPLE INTERNAL REFLECTION

IF $\theta > \theta_c$

θ_c DEPENDS ON REFRACTIVE INDEX OF THE TWO MEDIA WHERE REFLECTION TAKES PLACE.

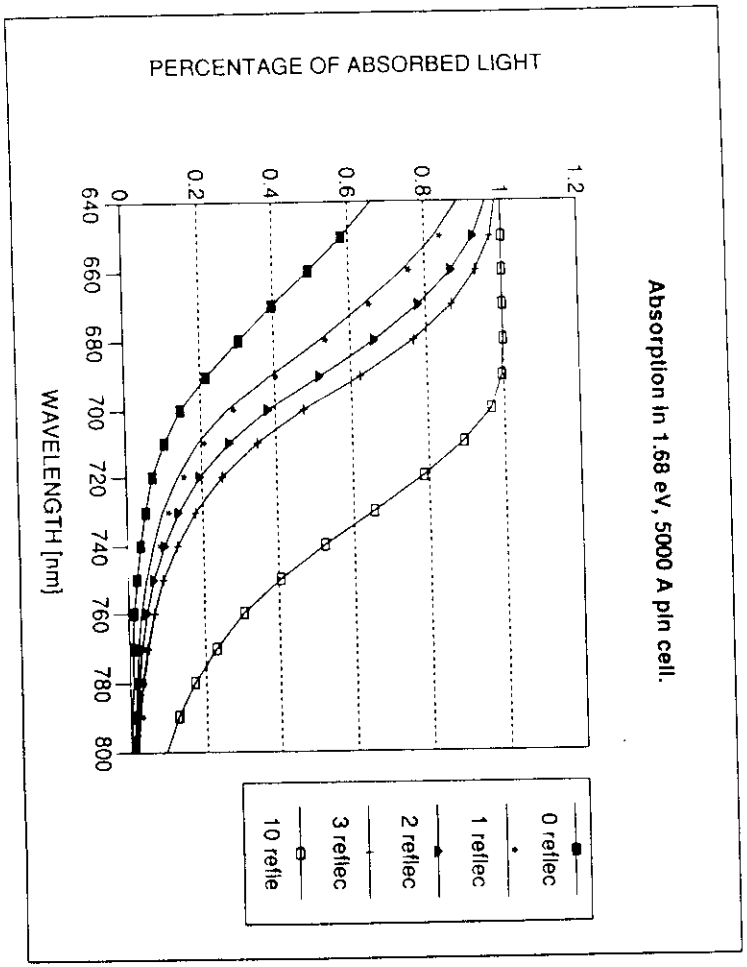

OUR METHOD OF TEXTURING

HOT SILVER	TEXTURE
ZNO	ADDITIONAL TEXTURE + BUFFER

THIS HAS GIVEN HIGH SHORT-CIRCUIT CURRENT.

HOW MUCH FURTHER IMPROVEMENT CAN WE GET?

a-SiGe alloy

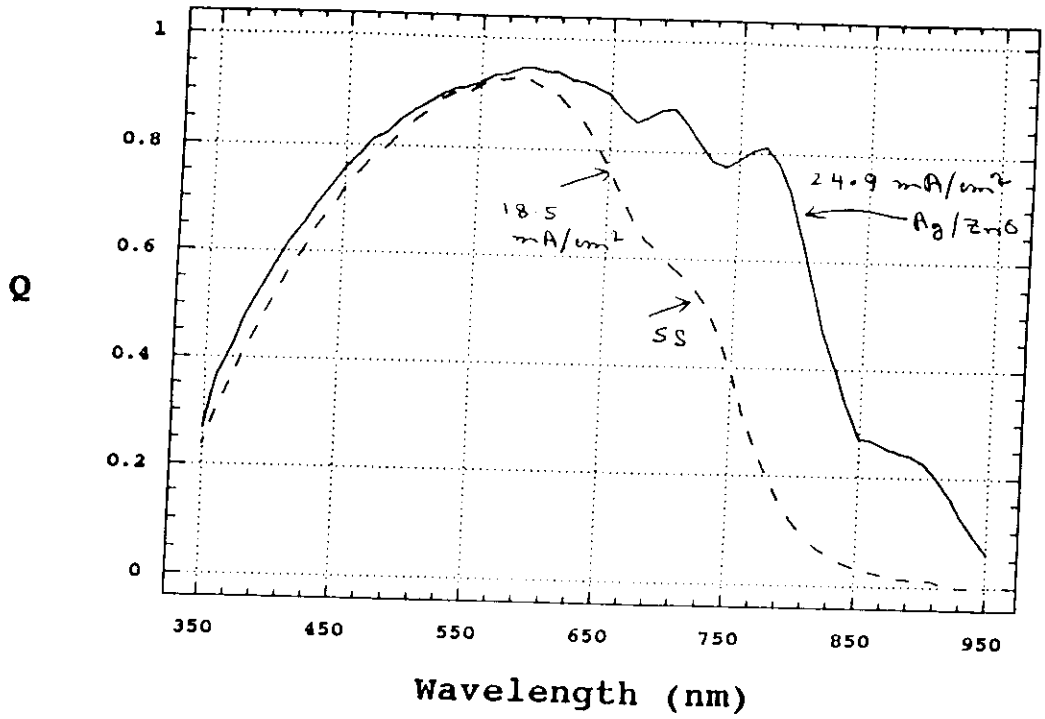

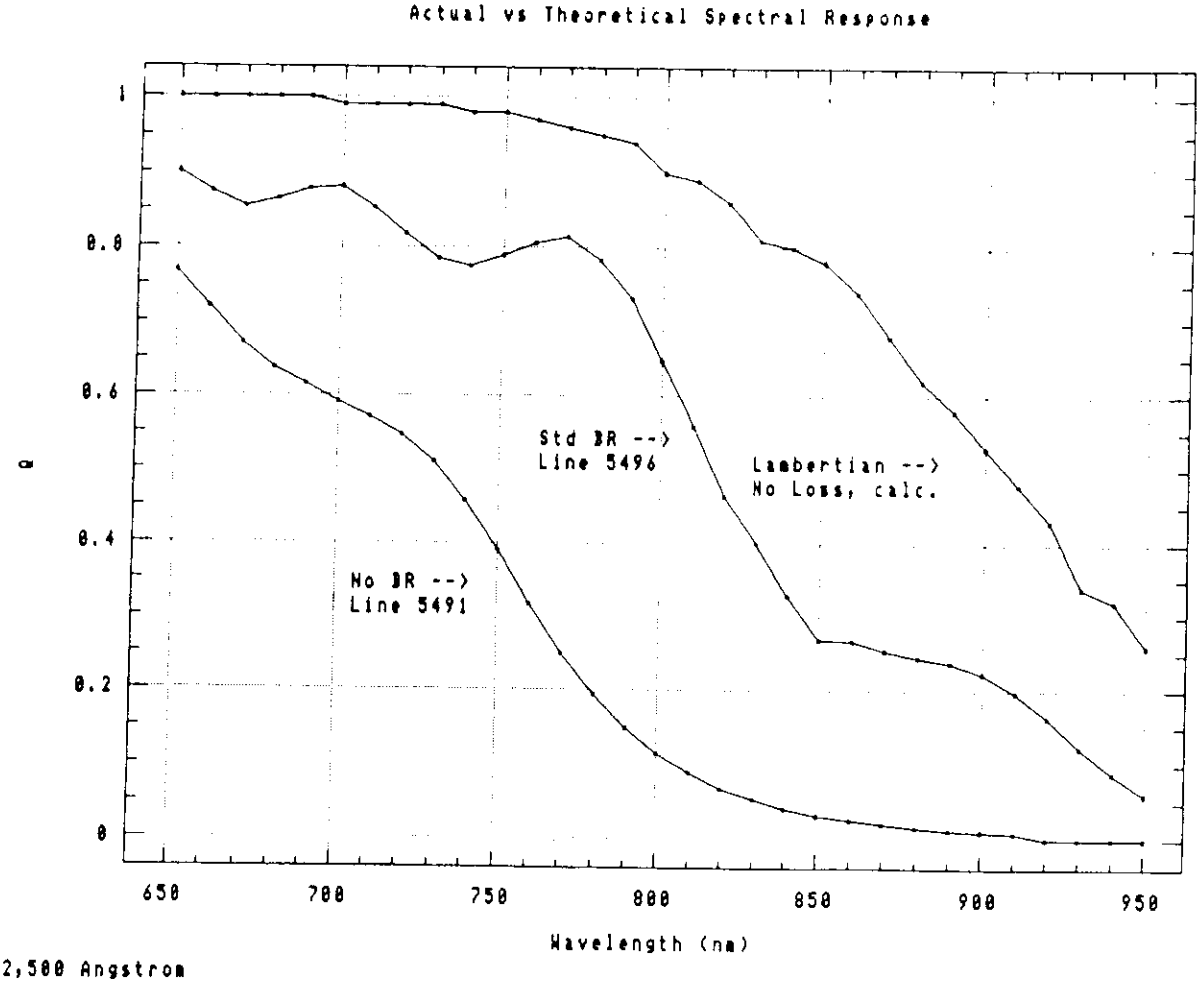

2,500 Angstrom

If you want photons of 630 nm to have total internal reflection, $\theta > \theta_c$

Ag/ZnO
Textured

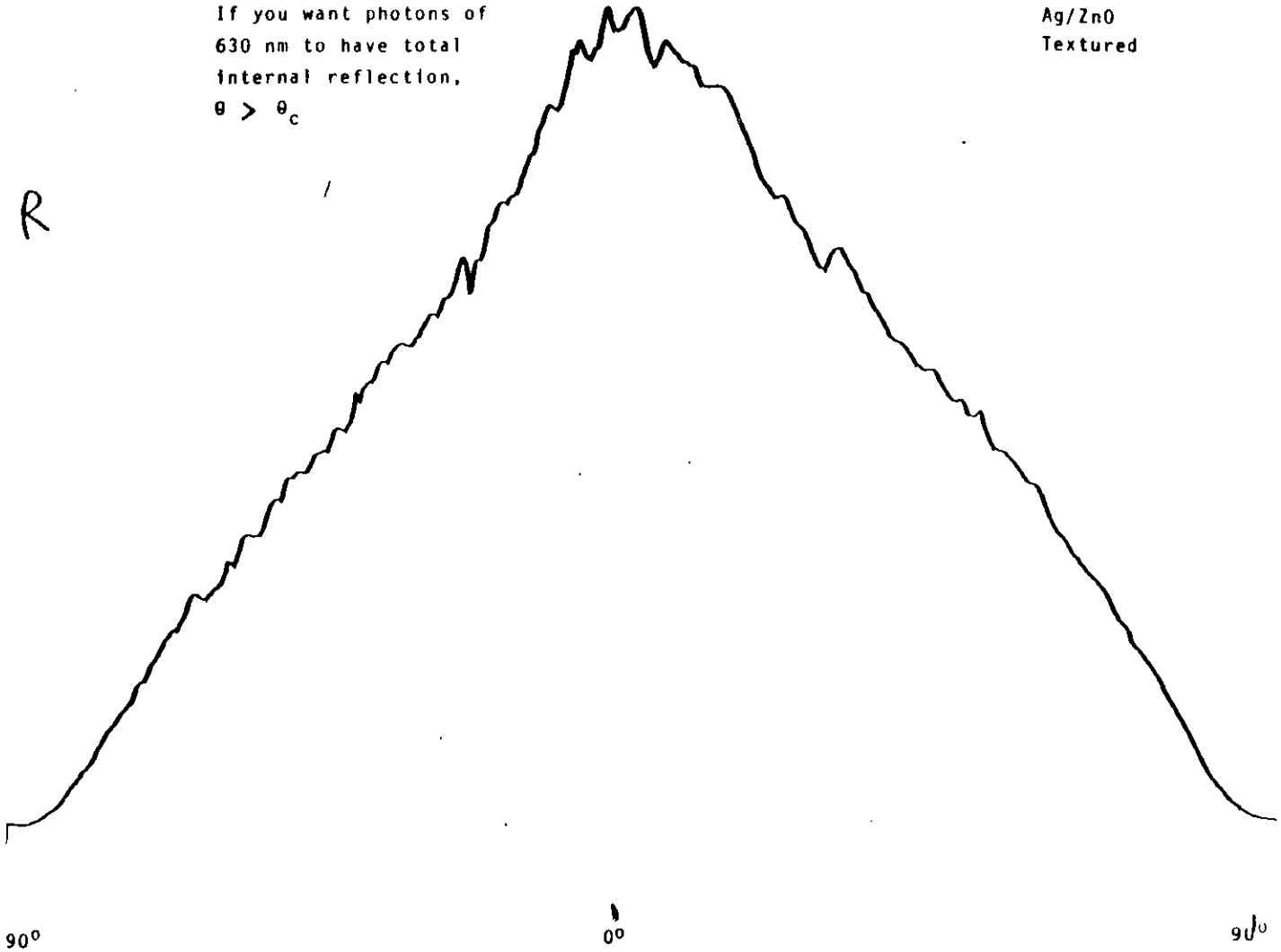

91

CHALLENGE

HOW TO MAKE A BACK REFLECTOR WHERE MOST OF THE LIGHT GETS REFLECTED AT A LARGE ANGLE?

92

BACK REFLECTOR A TYPE

WE CAN CHANGE θ_1 BY CHANGING THE TEXTURE

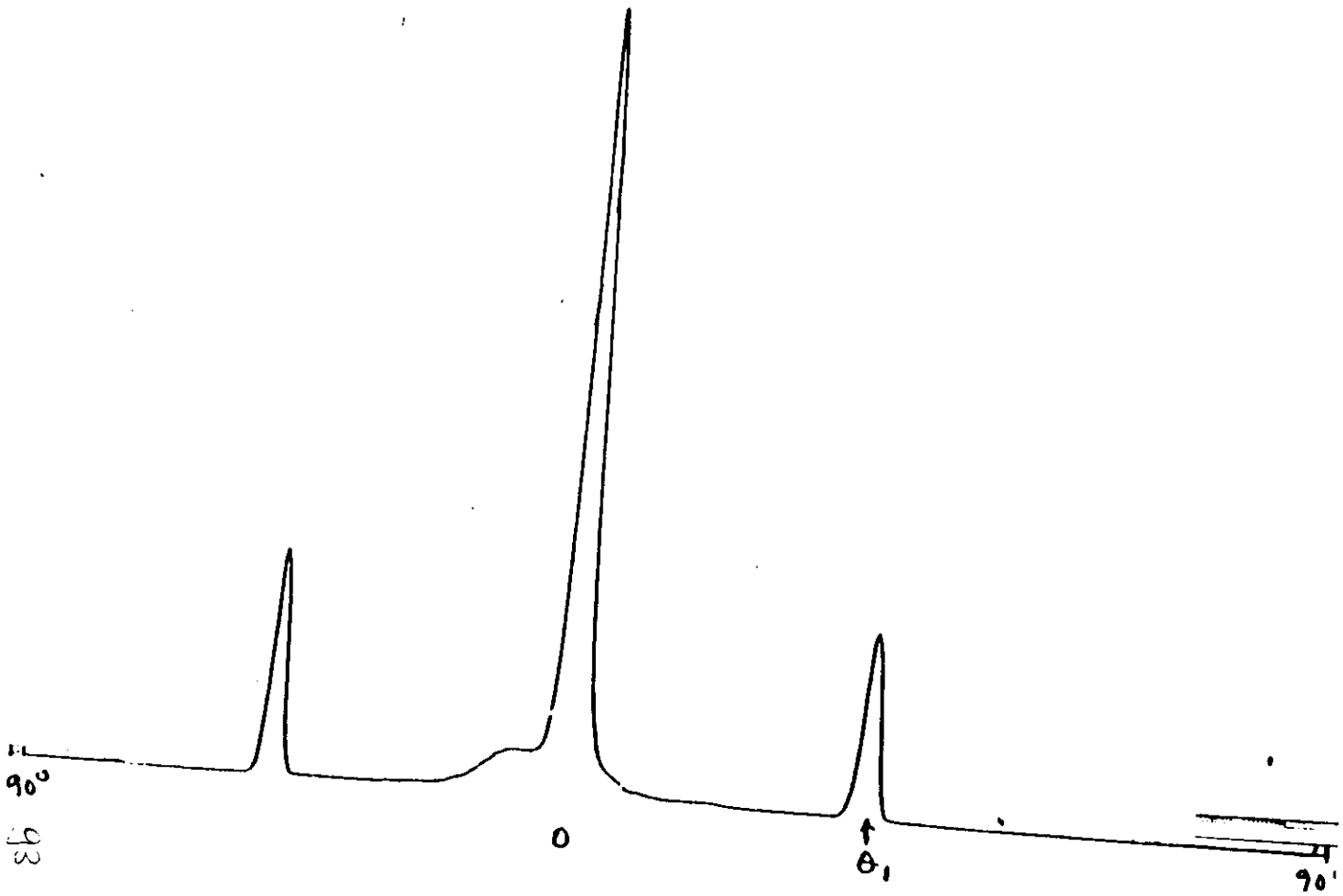

93

BACK REFLECTOR B TYPE

CONFIDENTIAL

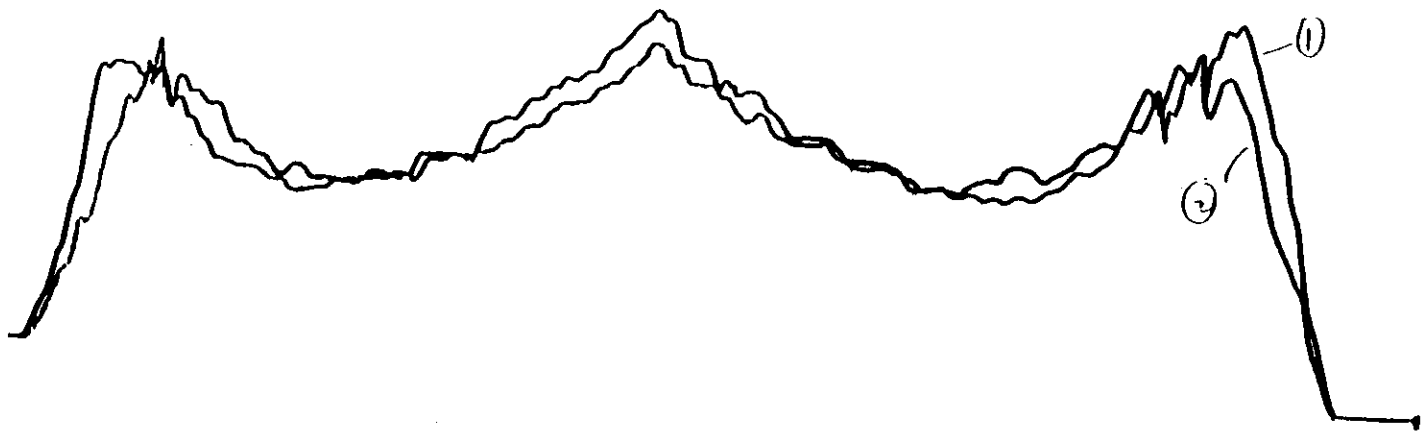

94

PROBLEM

AFTER OPTIMIZATION THE BEST J_{SC} VALUE FROM AG/ZNO IS THE SAME AS BR 'A' OR BR 'B'. SPECIALLY, LONG WAVELENGTH Q'S ARE IDENTICAL.

WHY?

- FINITE ABSORPTION LOSS IN ZINC OXIDE

- REFLECTION LOSS AT SILVER/ZINC OXIDE INTERFACE